

ARTICLE



<https://doi.org/10.1038/s41467-020-18367-y>

OPEN

Genetic correlations and genome-wide associations of cortical structure in general population samples of 22,824 adults

Edith Hofer et al.[#]

Cortical thickness, surface area and volumes vary with age and cognitive function, and in neurological and psychiatric diseases. Here we report heritability, genetic correlations and genome-wide associations of these cortical measures across the whole cortex, and in 34 anatomically predefined regions. Our discovery sample comprises 22,824 individuals from 20 cohorts within the Cohorts for Heart and Aging Research in Genomic Epidemiology (CHARGE) consortium and the UK Biobank. We identify genetic heterogeneity between cortical measures and brain regions, and 160 genome-wide significant associations pointing to *wnt/β-catenin*, *TGF-β* and *sonic hedgehog* pathways. There is enrichment for genes involved in anthropometric traits, hindbrain development, vascular and neurodegenerative disease and psychiatric conditions. These data are a rich resource for studies of the biological mechanisms behind cortical development and aging.

[#]A list of authors and their affiliations appears at the end of the paper.

The cortex is the largest part of the human brain, associated with higher brain functions, such as perception, thought, and action. Brain cortical thickness (CTh), cortical surface area (CSA), and cortical volume (CV) are morphological markers of cortical structure obtained from magnetic resonance imaging (MRI). These measures change with age^{1–3} and are linked to cognitive functioning^{4,5}. The human cortex is also vulnerable to a wide range of disease or pathologies, ranging from developmental disorders and early onset psychiatric and neurological diseases to neurodegenerative conditions manifesting late in life. Abnormalities in global or regional CTh, CSA, and CV have been observed in neurological and psychiatric disorders, such as Alzheimer's disease⁶, Parkinson's disease⁷, multiple sclerosis⁸, schizophrenia⁹, bipolar disorder⁹, depression¹⁰, and autism¹¹. The best method to study human cortical structure during life is using brain MRI. Hence, understanding the genetic determinants of the most robust MRI cortical markers in apparently normal adults could identify biological pathways relevant to brain development, aging, and various diseases. Neurons in the neocortex are organized in columns which run perpendicular to the surface of the cerebral cortex¹²; and, according to the radial unit hypothesis, CTh is determined by the number of cells within the columns and CSA is determined by the number of columns¹³.

Thus, CTh and CSA reflect different mechanisms in cortical development^{13,14} and are likely influenced by different genetic factors^{15–18}. CV, which is the product of CTh and CSA, is determined by a combination of these two measures, but the relative contribution of CTh and CSA to CV may vary across brain regions. CTh, CSA, and CV are all strongly heritable traits^{15–21} with estimated heritability of 0.69–0.81 for global CTh, and from 0.42 to 0.90 for global CSA^{15,16,18}. Across different cortical regions, however, there is substantial regional variation in heritability of CTh, CSA, and CV^{15–21}.

Since CTh, CSA, and CV are differentially heritable and genetically heterogeneous, we explore the genetics of each of these imaging markers using genome-wide association analyses (GWAS) in large population-based samples. We study CTh, CSA, and CV in the whole cortex and in 34 cortical regions in 22,824 individuals from 21 discovery cohorts and replicate the strongest associations in 22,363 persons from the Enhancing Neuroimaging Genetics through Meta-analysis (ENIGMA) consortium. Our analyses reveal 160 genome-wide significant associations pointing to *wnt*/ β -catenin, TGF- β , and sonic hedgehog pathways. We observe genetic heterogeneity between cortical measures and brain regions and find enrichment for genes involved in anthropometric traits, hindbrain development, vascular and neurodegenerative disease, and psychiatric conditions.

Results

Genome-wide association analysis. The analyses of global CTh, CSA, and CV included 22,163, 18,617, and 22,824 individuals, respectively. After correction for multiple testing ($p_{\text{Discovery}} < 1.09 \times 10^{-9}$), we identified no significant associations with global CTh. However, we identified 12 independent loci associated with global CSA ($n=6$) and CV ($n=6$). These are displayed in Supplementary Data 1 and Supplementary Figs. 1 and 2. Five of the 6 CSA loci were replicated in an external (ENIGMA consortium) sample²². The ENIGMA consortium only analyzed CSA and CTh.

GWAS of CTh, CSA, and CV in 34 cortical regions of interest (ROIs) identified 148 significant associations. There were 16 independent loci across 8 chromosomes determining CTh of 9 regions (Supplementary Data 2), 54 loci across 16 chromosomes associated with CSA of 21 regions (Supplementary Data 3), and 78 loci across 17 chromosomes determining CV of 23 cortical

regions (Supplementary Data 4). We replicated 57 out of 64 regional CTh and CSA loci that were available in the ENIGMA consortium sample²² using a conservative replication threshold of $p_{\text{Replication}} = 3.1 \times 10^{-4}$, 0.05/160. Region-specific variants with the strongest association at each genomic locus are shown in Tables 1–3. Chromosomal ideograms showing genome-wide significant associations with global and regional cortical measures in the discovery stage are presented in Fig. 1.

If we had used a more stringent threshold of $p_{\text{Discovery}} < 4.76 \times 10^{-10} = 5 \times 10^{-8}/105$, correcting for all the 105 GWAS analyses performed, we would have identified 142 significant associations (Supplementary Data 1–4).

The strongest associations with CTh and CV were observed for rs2033939 at 15q14 ($p_{\text{Discovery, CTh}} = 1.17 \times 10^{-73}$ and $p_{\text{Discovery, CV}} = 4.34 \times 10^{-133}$) in the postcentral (primary somatosensory) cortex, and for CSA with rs1080066 at 15q14 ($p_{\text{Discovery, CSA}} = 8.45 \times 10^{-109}$) in the precentral (primary motor) cortex. Figure 2 shows the lowest p-value of each cortical region. The postcentral cortex was also the region with the largest number of independent associations, mainly at a locus on 15q14. The corresponding regional association plots are presented in Supplementary Fig. 3. Quantile-quantile plots of all meta-analyses are presented in Supplementary Figs. 4–7 and the corresponding genomic inflation factors (λ_{GC}), LD score regression (LDSR) intercepts, and ratios are shown in Supplementary Data 5. Although we observe inflated test statistics for some traits with λ_{GC} between 1.02 and 1.11, LDSR intercepts between 0.98 and 1.02 indicate that the inflation is mainly due to polygenicity. For traits with $\lambda_{\text{GC}} > 1.05$, the LDSR ratios range between 0.00 and 0.15 which means that a maximum of 15% of the inflation is due to other causes.

Associations across cortical measures and with other traits.

Supplementary Data 6 presents variants that are associated with the CSA or the CV across multiple regions. We observed 25 single nucleotide polymorphisms (SNPs) that determined both the CSA and CV of a given region, 4 SNPs that determined CTh and CV of the same region, but no SNPs that determined both the CTh and CSA of any given region (Supplementary Data 7). We also checked the overlap between our findings and two previous GWAS studies, including 8428²³ and 19,621²⁴ individuals from the UK Biobank, which among other phenotypes, investigate CTh, CSA, and CV (Supplementary Data 8). Regarding CTh, one variant, rs2033939 at 15q14, was associated with CTh of the postcentral gyrus in both studies. For CSA and CV, we found 11 associations at 15q14, 14q23.1 and 3q24, and 14 associations at 15q14, 14q23.1, 3q24, 8q24.1, 12q14.3, and 20q13.2, respectively, with the same cortical region as in our study. Out-of-sample polygenic risk score (PRS) analyses showed associations ($p_{\text{PRS}} < 4.76 \times 10^{-3}$) with all investigated cortical measures in all cortical regions in 7800 UK Biobank individuals (Supplementary Data 9). For CTh, we observed the maximum phenotypic variance explained by the PRS (R_{PRS}^2) in the global cortex ($R_{\text{PRS}}^2 = 0.015$, $p_{\text{PRS}} = 1.05 \times 10^{-26}$), and for CSA and CV in the pericalcarine cortex ($R_{\text{PRS}^2\text{-CSA}} = 0.029$, $p_{\text{PRS,CSA}} = 1.29 \times 10^{-50}$; $R_{\text{PRS}^2\text{-CV}} = 0.032$, $p_{\text{PRS,CV}} = 5.30 \times 10^{-56}$). When assessing genetic overlap with other traits, we observed that SNPs determining these cortical measures have been previously associated with anthropometric (height), neurologic (Parkinson's disease, corticobasal degeneration, and Alzheimer's disease), psychiatric (neuroticism and schizophrenia) and cognitive performance traits as well as with total intracranial volume (TIV) on brain MRI (Supplementary Data 10–12).

Gene identification. Positional mapping based on ANNOVAR showed that most of the lead SNPs were intergenic and intronic

Table 1 Genome-wide significant associations ($p_{\text{Discovery}} < 1.09 \times 10^{-9}$) of regional CTh.

Lobe	Region	Locus	Position	Lead SNP	Nearest gene	Annotation	N	$p_{\text{Discovery}}$	Replication	p_{Pooled}
Temporal	Superior temporal	16q24.2	87225139	rs4843227	LOC101928708	Intergenic	21,887	2.79E-12	2.45E-05	2.31E-15
	Middle temporal	17q21.31	44861003	rs199504	WNT3	Intronic	21,887	1.30E-10	1.17E-04	5.85E-13
	Inferior temporal	14q23.1	59072144	rs10782438	KIAA0586	Intergenic	21,559	2.17E-13	2.76E-08	8.99E-21
	Banksts	2q35	217332057	rs284532	SMARCAL1	Intronic	21,885	1.03E-09	2.64E-01	3.04E-07
Parietal	Superior parietal	14q23.1	59074878	rs160458	KIAA0586C	Intergenic	18,342	9.39E-10	2.42E-09	6.45E-18
		16q24.2	87225101	rs9937293	LOC101928708	Intergenic	21,886	2.68E-14	1.64E-13	2.27E-27
		1q41	215141570	rs10494988	CNK2	Intergenic	21,886	2.60E-12	3.66E-08	2.63E-19
Occipital	Postcentral	15q14	39633904	rs2033939	C1orf54	Intergenic	21,885	1.17E-11	5.18E-06	7.73E-136
	Lateral occipital	5q14.1	79933093	rs245100	DHFR	Intronic	21,886	2.68E-11	3.77E-06	1.16E-15
	Cuneus	14q23.1	59624317	rs4901904	DAAMI	Intergenic	21,885	4.02E-14	3.17E-10	2.88E-23
	Insula	16q12.1	51449978	rs7197215	SALL1	Intergenic	21,560	1.45E-13	2.00E-02	6.42E-12
		9q31.3	113679617	rs72748157	LPARI	Intronic	21,560	1.46E-10	1.38E-04	5.16E-13

N number of individuals in meta-analysis, $p_{\text{Discovery}}$ two-sided p-value of discovery GWAS meta-analysis in CHARGE, $p_{\text{Replication}}$ two-sided p-value of replication meta-analysis in ENIGMA, p_{Pooled} two-sided p-value of pooled discovery and replication meta-analysis, p-values are not adjusted for multiple comparisons, *banksts* banks of the superior temporal sulcus.

in bold: significant replication— $p_{\text{Replication}} < 3.1 \times 10^{-4}$ ($= 0.05/N$, $N=160$, total number of lead SNPs).

(Fig. 3). One variant, rs2279829, which was associated with both CSA and CV of the pars triangularis, postcentral and supra-marginal cortices, is located in the 3'UTR of *ZIC4* at 3q24. We also found an exonic variant, rs10283100, in gene *ENPP2* at 8q24.12 associated with CV of the insula.

We used multiple strategies beyond positional annotation to identify specific genes implicated by the various GWAS associated SNPs. FUMA identified 232 genes whose expression was determined by these variants (eQTL) and these and other genes implicated by chromatin interaction mapping are shown in Supplementary Data 13–15. MAGMA gene-based association analyses revealed 70 significantly associated ($p < 5.87 \times 10^{-8}$) genes (Supplementary Data 16–18). For global CSA and CV, 7 of 9 genes associated with each measure overlapped, but there was no overlap with global CTh. For regional CSA and CV, we found 28 genes across 13 cortical regions that determined both measures in the same region. Figure 4 summarizes the results of GTEx eQTL, chromatin interaction, positional annotation, and gene-based mapping strategies for all regions. While there are overlapping genes identified using different approaches, only *DAAMI* gene (Chr14q23.1) is identified by all types of gene mapping for CV of insula. eQTL associations of our independent lead SNPs in the Religious Orders Study Memory and Aging Project (ROSMAP) dorsolateral frontal cortex gene expression dataset are presented in Supplementary Data 19.

Pathway analysis. MAGMA gene set analyses identified 7 pathways for CTh, 3 pathways for CSA and 9 pathways for CV (Supplementary Data 20). Among them are the gene ontology (GO) gene sets hindbrain morphogenesis (strongest association with thickness of middle temporal cortex), forebrain generation of neurons (with surface area of precentral cortex), and central nervous system neuron development (with volume of transverse temporal cortex). However, after Bonferroni correction only one significant pathway ($p < 1.02 \times 10^{-7}$) remained: regulation of catabolic process for CTh of the inferior temporal cortex. InnateDB pathway analyses of genes mapped to independent lead SNPs by FUMA showed a significant overlap between CTh and CSA genes and the Wnt signaling pathway (Supplementary Figs. 8 and 9) as well as a significant overlap between CV genes and the basal cell carcinoma pathway (Supplementary Fig. 10).

Heritability. Heritability estimates (h^2) of global CTh were 0.64 (standard error (se) = 0.12; $p_{\text{SOLAR}} = 3 \times 10^{-7}$) in the ASPS-Fam study and 0.45 (se = 0.08; $p_{\text{GCTA}} = 2.5 \times 10^{-7}$) in the Rotterdam study (RS). For CSA, h^2 was 0.84 (se = 0.12; $p_{\text{SOLAR}} = 2.63 \times 10^{-11}$) in ASPS-Fam and 0.33 (se = 0.08, $p_{\text{GCTA}} = 1 \times 10^{-4}$) in RS, and for CV, h^2 was 0.80 (se = 0.11; $p_{\text{SOLAR}} = 1.10 \times 10^{-9}$) in ASPS-Fam and 0.32 (se = 0.08; $p_{\text{GCTA}} = 1 \times 10^{-4}$) in RS. There was a large range in heritability estimates of regional CTh, CSA, and CV (Supplementary Data 21).

Heritability based on common SNPs as estimated with LDSR was 0.25 (se = 0.03) for global CTh, 0.29 (se = 0.04) for global CSA and 0.30 (se = 0.03) for global CV. LDSR heritability estimates of regional CTh, CSA, and CV are presented in Supplementary Data 21 and Supplementary Fig. 11. For the regional analyses, the estimated heritability ranged from 0.05 to 0.18 for CTh, from 0.07 to 0.36 for CSA and from 0.06 to 0.32 for CV. Superior temporal cortex ($h^2_{\text{CTh}} = 0.18$, $h^2_{\text{CSA}} = 0.30$, $h^2_{\text{CV}} = 0.26$), precuneus ($h^2_{\text{CTh}} = 0.16$, $h^2_{\text{CSA}} = 0.29$, $h^2_{\text{CV}} = 0.28$) and pericalcarine ($h^2_{\text{CTh}} = 0.15$, $h^2_{\text{CSA}} = 0.36$, $h^2_{\text{CV}} = 0.32$) are among the most genetically determined regions.

The results of partitioned heritability analyses for global and regional CTh, CSA, and CV with functional annotation and additionally with cell-type-specific annotation are presented in

Table 2 Genome-wide significant associations ($P_{\text{Discovery}} < 1.09 \times 10^{-9}$) of global and regional CSA.

Lobe	Region	Locus	Position	Lead SNP	Nearest gene	Annotation	N	$P_{\text{Discovery}}$	$P_{\text{Replication}}$	P_{Pooled}
Frontal	Global	17q21.31	44787313	rs538628	NSF	Intronic	18,617	1.78E-23	4.45E-22	1.00E-43
		6q22.32	126792095	rs11759026	MIR588	Intergenic	18,617	5.21E-22	1.45E-14	3.50E-34
		6q22.33	127204623	rs9375477	RPO3	Intergenic	18,617	4.86E-13	1.60E-08	1.23E-19
		6q21	1090000316	rs9398173	FOXO3	Intronic	18,617	6.84E-10	2.96E-03	2.05E-10
		5q14.3	92187932	rs17669337	NZF1-AS1	Intergenic	18,272	1.40E-11	NA	8.07E-16
		6q22.32	126876580	rs9388500	RPO3	Intergenic	17,891	2.35E-11	NA	NA
		5q23.3	128734008	rs12187568	ADAMTS19	Intergenic	16,632	1.19E-16	NA	NA
		3q24	147106319	rs2279829	ZIC4	UTR3	18,265	6.32E-20	1.94E-27	1.20E-45
		7q21.3	96175094	rs10458281	LOC100506136	Intergenic	18,265	1.15E-17	2.42E-11	1.20E-26
		15q14	39634222	rs1080066	C15orf54	Intergenic	18,267	8.45E-109	2.53E-95	1.00E-200
Temporal	Superior temporal	6q15	92002569	rs9345124	MAP3K7	Intergenic	18,267	5.50E-11	2.73E-14	9.91E-24
		2p16.3	48274592	rs386645843	FBXO1	Intergenic	18,269	9.51E-12	8.42E-07	1.71E-16
		4q26	119249835	rs5569931	PRSS12	Intronic	18,269	2.08E-10	2.72E-02	6.96E-10
		2q23.2	150022681	rs13008194	LYPD6B	Intronic	18,269	5.94E-11	2.54E-07	1.92E-16
		6q22.32	126964510	rs4273712	RPO3	Intergenic	18,269	6.93E-10	1.07E-04	1.99E-12
		14q23.1	59072226	rs186347	KIAA0386	Intergenic	18,265	4.11E-10	1.83E-09	4.93E-18
		17q21.31	44822662	rs199535	NSF	Intronic	18,265	1.01E-13	1.14E-06	8.13E-18
		2p25.2	150012936	rs2046268	LYPD6B	Intronic	18,264	9.09E-10	3.21E-10	1.78E-18
		15q14	39632013	rs71471500	C15orf54	Intergenic	18,270	3.85E-24	5.55E-19	5.88E-41
		19p13.2	13109763	rs68175985	NFIX	Intronic	17,324	8.84E-11	2.68E-17	2.90E-26
Parietal	Inferior parietal	20q13.2	52448936	rs6097618	SJMO1P1	Intergenic	18,267	1.78E-16	NA	NA
		12q14.3	65797096	rs2336713	MSRB3	Intronic	18,267	1.24E-12	2.99E-12	2.85E-23
		2p25.2	4563477	rs6669952	LINC01249	Intergenic	18,267	4.47E-10	1.37E-08	4.73E-17
		15q14	39633904	rs2033939	C15orf54	Intergenic	18,272	9.07E-27	1.61E-28	1.59E-53
		14q23.1	59627631	rs2164950	DAAM1	Intergenic	18,272	1.25E-13	3.79E-14	3.46E-26
		3q24	147106319	rs2279829	ZIC4	UTR3	18,272	7.38E-12	4.24E-16	2.29E-26
		15q14	39634222	rs1080066	C15orf54	Intergenic	18,265	5.65E-47	2.44E-36	1.87E-80
		3q24	147106319	rs2279829	ZIC4	UTR3	18,265	1.90E-21	1.69E-26	2.92E-46
		9q21.13	76144318	rs67286026	ANXA1	Intergenic	18,265	3.58E-12	8.04E-06	7.82E-16
		14q23.1	59628609	rs74826997	DAAM1	Intronic	18,270	2.40E-24	4.41E-18	4.59E-40
Occipital	Lateral occipital	6q23.3	138866268	rs9376354	NHS1	Intergenic	18,270	7.80E-13	4.12E-08	7.28E-19
		3q26	190666643	rs1159211	SNAR-1	Intergenic	18,270	4.49E-10	2.04E-05	1.59E-13
		14q23.1	59627631	rs2164950	DAAM1	Intergenic	18,269	3.04E-26	2.92E-15	2.25E-38
		14q23.1	59628679	rs76341705	DAAM1	Intergenic	18,270	1.57E-20	8.67E-13	9.96E-31
		14q23.1	59625997	rs73313052	DAAM1	Intergenic	18,267	1.90E-32	3.19E-15	2.96E-43
		13q31.1	80191873	rs9545155	LINC01038	Intergenic	18,267	5.15E-10	2.98E-05	3.91E-13
		14q23.1	59628679	rs76341705	DAAM1	Intergenic	18,267	4.67E-24	2.56E-19	3.35E-41
		5q12.1	60117723	rs6893642	ELOVL7	Intronic	18,267	1.40E-13	1.68E-08	6.29E-20
		3q13.1	104724787	rs971550	ALCAM	Intergenic	18,267	2.18E-10	1.31E-06	4.49E-15
		6q22.33	127185801	rs9375476	RPO3	Intergenic	18,267	2.20E-10	2.24E-08	4.32E-17
Posterior cingulate	Insula	1p13.2	113239478	rs2999158	MOV10	Intronic	18,267	6.46E-10	8.39E-10	3.49E-18
		13q31.1	80191873	rs9545155	LINC01068	Intergenic	18,267	7.51E-10	7.53E-09	4.05E-17
		5q12.3	66104105	rs17214309	MAS74	Intronic	18,268	7.84E-11	1.52E-05	4.04E-14
		10q25.3	118704077	rs1905544	SHTN1	Intronic	17,599	4.06E-12	3.65E-03	1.28E-11

N number of individuals in meta-analysis, $P_{\text{Discovery}}$ two-sided p-value of discovery GWAS meta-analysis in ENIGMA, P_{Pooled} two-sided p-value of replication meta-analysis in ENIGMA, $P_{\text{Replication}}$ two-sided p-value of replication meta-analysis and replication meta-analysis, p-values are not adjusted for multiple comparisons, *banksts* banks of the superior temporal sulcus. NA, SNP or region not available in the ENIGMA sample. In bold: significant replication— $P_{\text{Replication}} < 3.1 \times 10^{-4}$ ($\alpha = 0.05/N_I$, $N_I = 160$, total number of lead SNPs).

Table 3 Genome-wide significant associations ($p_{\text{Discovery}} < 1.09 \times 10^{-9}$) of global and regional CV.

Lobe	Region	Locus	Position	Lead SNP	Nearest gene	Annotation	N	$P_{\text{Discovery}}$	
Frontal	Global	6q22.32	126792095	rs11759026	MIR588	Intergenic	22,410	6.31E-19	
		17q21.31	44790203	rs169201	NSF	Intronic	22,784	2.11E-13	
		17q21.32	43549608	rs149366495	PLEKHM1	Intronic	22,099	8.18E-13	
		12q14.3	66358347	rs1042725	HMGA2	3'UTR	22,784	7.04E-11	
		12q23.2	102921296	rs11111293	IGF1	Intergenic	22,784	5.45E-10	
	Superior frontal	6q22	109002042	rs4945816	FOXO3	3'UTR	22,784	8.93E-10	
		5q14.3	92186429	rs888814	NR2F1-AS1	Intergenic	22,692	3.29E-13	
		15q14	39636227	rs17694988	C15orf54	Intergenic	22,793	3.15E-11	
		2q12.1	105460333	rs745249	LINC01158	ncRNA_intronic	22,726	2.35E-11	
		6q22.32	127068983	rs853974	RSPO3	Intergenic	22,351	4.82E-11	
		Pars opercularis	5q23.3	128734008	rs12187568	ADAMTS19	Intergenic	20,753	4.27E-18
			15q14	39639898	rs4924345	C15orf54	Intergenic	22,758	1.97E-14
		Pars triangularis	3q24	147106319	rs2279829	ZIC4	UTR3	22,759	3.16E-23
			7q21.3	96196906	rs67055449	LOC100506136	Intergenic	22,759	4.03E-19
			15q14	39633904	rs2033939	C15orf54	Intergenic	22,759	8.49E-14
Temporal	Lateral orbitofrontal	7q21.3	96129071	rs62470042	C7orf76	Intronic	22,759	7.38E-13	
		6q15	91942761	rs12660096	MAP3K7	Intergenic	22,759	4.74E-10	
		14q22.2	54769839	rs6572946	CDKN3	Intergenic	22,801	2.29E-10	
	Precentral	15q14	39634222	rs1080066	C15orf54	Intergenic	22,699	5.84E-125	
		10q25.3	118648841	rs3781566	SHTN1	Intronic	22,699	4.68E-11	
	Superior temporal	3q26.32	177296448	rs13084960	LINC00578	ncRNA_intronic	22,681	1.12E-11	
		14q23.1	59072226	rs186347	KIAA0586	Intergenic	22,727	1.15E-15	
	Fusiform	14q23.1	59833172	rs1547199	DAAM1	Intronic	22,605	4.58E-10	
		1p33	47980916	rs6658111	FOXD2	Intergenic	22,605	7.78E-10	
	Transverse temporal	2q23.2	150012936	rs2046268	LYPD6B	Intronic	22,786	2.55E-12	
		2q33.1	199809716	rs966744	SATB2	Intergenic	22,747	2.23E-10	
	Parietal	Superior parietal	15q14	39633904	rs2033939	C15orf54	Intergenic	22,723	4.28E-23
			16q24.2	87225139	rs4843227	LOC101928708	Intergenic	22,723	1.16E-13
		Inferior parietal	19p13.2	13109763	rs68175985	NFIX	Intronic	21,777	3.27E-11
			5q15	92866553	rs62369942	NR2F1-AS1	ncRNA_intronic	21,664	4.32E-10
Supramarginal		20q13.2	52448936	rs6097618	SUMO1P1	Intergenic	22,701	2.09E-17	
		12q14.3	65797096	rs2336713	MSRB3	Intronic	22,701	2.47E-13	
		3q13.11	104724634	rs971551	ALCAM	Intergenic	22,701	2.34E-10	
Postcentral		15q14	39632013	rs71471500	THBS1	Intergenic	22,645	9.71E-28	
		14q23.1	59627631	rs2164950	DAAM1	Intergenic	22,645	3.59E-20	
Occipital		Precuneus	3q24	147106319	rs2279829	ZIC4	UTR3	22,645	5.36E-18
			15q14	39633904	rs2033939	THBS1	Intergenic	22,662	4.34E-133
			3q24	147106319	rs2279829	ZIC4	UTR3	22,662	2.54E-17
		Lateral occipital	9q21.13	76144318	rs67286026	ANXA1	Intergenic	22,662	5.03E-11
			2q36.3	226563259	rs16866701	NYAP2	Intergenic	22,545	5.69E-11
		Lingual	14q23.1	59627631	rs2164950	DAAM1	Intergenic	22,803	4.85E-20
	3q28		190663557	rs35055419	OSTN	Intergenic	22,428	2.02E-10	
	Cuneus	2p22.2	37818236	rs2215605	CDC42EP3	Intergenic	22,803	3.43E-10	
		3q13.11	104713881	rs12495603	ALCAM	Intergenic	22,803	9.71E-10	
	Pericalcarine	14q23.1	59625997	rs73313052	DAAM1	Intergenic	22,799	6.89E-16	
		6q22.32	127089401	rs2223739	RSPO3	Intergenic	22,805	1.75E-10	
	Insula	Caudal anterior cingulate	14q23.1	59625997	rs73313052	DAAM1	Intergenic	22,799	4.59E-43
			11p15.3	12072213	rs11022131	DKK3	Intergenic	22,799	5.96E-12
		Insula	13q31.1	80192236	rs9545156	LINC01068	Intergenic	22,799	4.09E-10
			14q23.1	59628679	rs76341705	DAAM1	Intergenic	22,824	1.39E-29
Insula		13q31.1	80191873	rs9545155	LINC01068	Intergenic	22,824	2.25E-13	
		11p14.1	30876113	rs273594	DCDC5	Intergenic	22,824	3.51E-13	
Insula		1p13.2	113208039	rs12046466	CAPZA1	Intronic	22,824	2.36E-12	
		1p33	47980916	rs6658111	FOXD2	Intergenic	22,824	3.85E-11	
Insula		11q22.3	104012656	rs1681464	PDGFD	Intronic	22,824	7.51E-11	
		6q22.32	127096181	rs9401907	RSPO3	Intergenic	22,824	2.11E-10	
Insula		7p21.1	18904400	rs12700001	HDAC9	Intronic	22,824	2.12E-10	
		5q12.1	60315823	rs10939879	NDUFAF2	Intronic	22,824	2.92E-10	
Insula		5q14.3	82852578	rs309588	VCAN	Intronic	22,748	2.60E-10	
		11q23.1	110949402	rs321403	C11orf53	Intergenic	22,543	9.58E-12	
Insula		8q24.12	120596023	rs10283100	ENPP2	Exonic	21,481	8.29E-11	

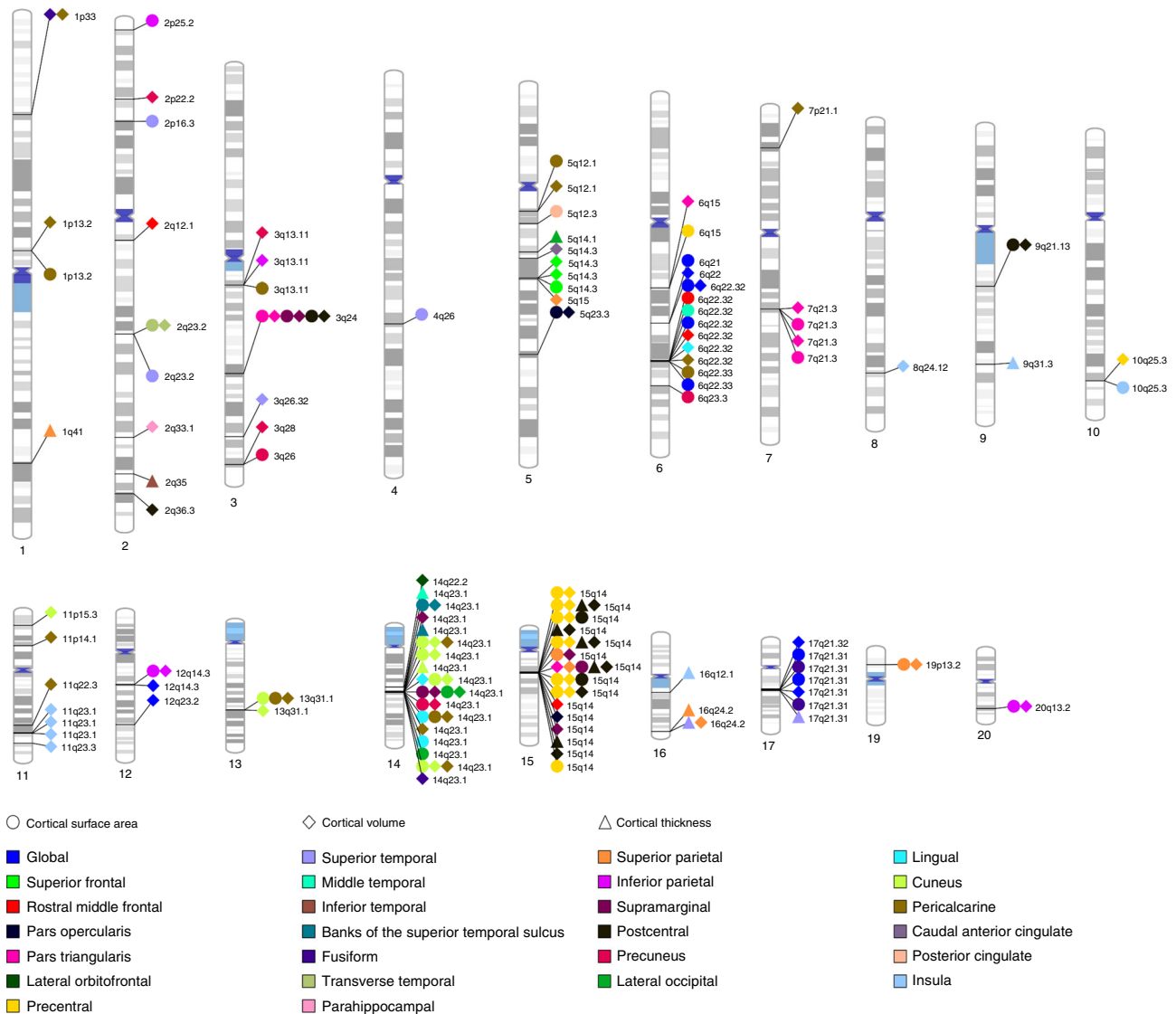


Fig. 1 Chromosomal ideogram of genome-wide significant associations with measures of cortical structure. Cortical surface areas, cortical volumes and cortical thickness. Each point represents the significantly associated variant, the colors correspond to the different cortical regions and the shape to different type of measurement ($p_{\text{Discovery}} < 1.09 \times 10^{-9}$).

Supplementary Data 22 and 23. For global CTh, we found enrichment for super-enhancers, introns and histone marks. Repressors and histone marks were enriched for global CSA, and introns, super-enhancers, and repressors for global CV. For regional CSA and CV the highest enrichment scores (>18) were observed for conserved regions.

Genetic correlation. We found high genetic correlation (r_g) between global CSA, and global CV ($r_g = 0.81$, $p_{\text{LDSCR}} = 1.2 \times 10^{-186}$) and between global CTh and global CV ($r_g = 0.46$, $p_{\text{LDSCR}} = 1.4 \times 10^{-14}$), but not between global CTh and global CSA ($r_g = -0.02$, $p_{\text{LDSCR}} = 0.82$). Whereas the genetic correlation between CSA and CV was strong ($r_g > 0.7$) in most of the regions (Supplementary Data 24 and Supplementary Fig. 12), it was generally weak between CSA and CTh with $r_g < 0.3$, and ranged from 0.09 to 0.69 between CTh and CV. The postcentral and lingual cortices were the two regions with the highest genetic correlations between both CTh and CV, as well as CTh and CSA.

Genetic correlation across the various brain regions for CTh (Supplementary Fig. 13, Supplementary Data 25), CSA (Supplementary Fig. 14, Supplementary Data 26), and CV

(Supplementary Fig. 15, Supplementary Data 27) showed a greater number of correlated regions for CTh and greater inter-regional variation for CSA and CV. Supplementary Data 28–30 and Supplementary Figs. 16–18 show genome-wide genetic correlations between the cortical measures and anthropometric, neurological and psychiatric, and cerebral structural traits.

Discussion

In our genome-wide association study of up to 22,824 individuals for MRI determined cortical measures of global and regional thickness, surface area, and volume, we identified 160 genome-wide significant associations across 19 chromosomes. Heritability was generally higher for cortical surface area and volume than for thickness, suggesting a greater susceptibility of cortical thickness to environmental influences. We observed strong genetic correlations between surface area and volume, but weak genetic correlation between surface area and thickness. We identified the largest number of novel genetic associations with cortical volumes, perhaps due to our larger sample size for this phenotype, which was assessed in all 21 discovery samples.

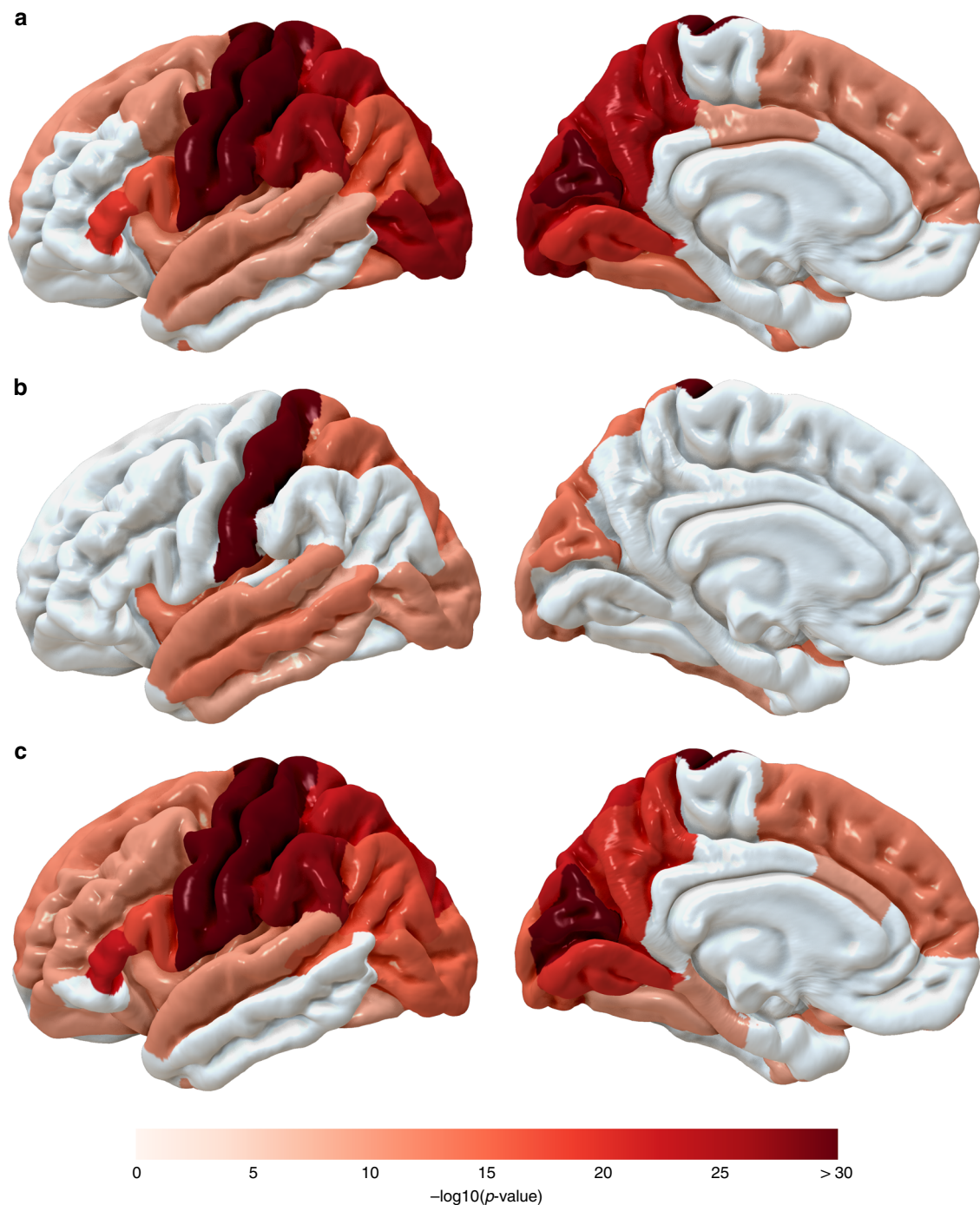


Fig. 2 Lowest discovery meta-analysis p -value of CSA, CTh, and CV in each cortical region. **a** Lowest $p_{\text{Discovery}}$ of CSA, **b** lowest $p_{\text{Discovery}}$ of CTh, **c** lowest $p_{\text{Discovery}}$ of CV.

It is beyond the scope of our study to discuss each of the 160 associations identified. A large number of the corresponding genes are involved in pathways that regulate morphogenesis of neurons, neuronal cell differentiation, and cell growth, as well as cell migration and organogenesis during embryonic development. At a molecular level, the wnt/β -catenin, TGF- β , and sonic hedgehog pathways are strongly implicated. Gene-set-enrichment analyses revealed biological processes related to brain morphology and neuronal development.

Broad patterns emerged showing that genes determining cortical structure are also often implicated in development of the cerebellum and brainstem (*KIAA0586*, *ZIC4*, *ENPP2*) as well as

the neural tube (one carbon metabolism genes *DHFR* and *MSRBB3*, the latter also associated with hippocampal volumes²⁵). These genes determine development of not only neurons but also astroglia (*THBS1*) and microglia (*SALL1*). They determine susceptibility or resistance to a range of insults: inflammatory, vascular (*THBS1*, *ANXA1*, *ARRDC3-AS1*²⁶) and neurodegenerative (*C15orf53*, *ZIC4*, *ANXA1*), and have been associated with pediatric and adult psychiatric conditions (*THBS1*).

There is a wealth of information in the supplementary tables that can be mined for a better understanding of brain development, connectivity, function and pathology. We highlight this potential by discussing in additional detail, the possible

significance of 6 illustrative loci, 5 of which, at 15q14, 14q23.1, 6q22.32, 17q21.31, and 3q24, associate with multiple brain regions at low p -values, while the locus at 8q24.12 identifies a plausible exonic variant.

The Chr15q14 locus was associated with cortical thickness, surface area, and volumes in the postcentral gyrus as well as with surface area or volume across six other regions in the frontal and parietal lobes. Lead SNPs at this locus were either intergenic between *C15orf53* and *C15orf54*, or intergenic between *C15orf54* and *THBS1* (Thrombospondin-1). *C15orf53* has been associated with an autosomal recessive form of spastic paraplegia showing intellectual disability and thinning of the corpus callosum (hereditary spastic paraparesis 11, or Nakamura Osame syndrome). Variants of *THBS1* were reported to be related to autism²⁷ and schizophrenia²⁸. The protein product of *THBS1* is involved in astrocyte induced synaptogenesis²⁹, and regulates chain migration of interneuron precursors migrating in the postnatal radial migration stream to the olfactory bulb³⁰. Moreover, *THBS1* is an activator of TGF β signaling, and an inhibitor of pro-angiogenic nitric oxide signaling, which plays a role in several cancers and immune-inflammatory conditions.

Variants at Chr14q23.1 were associated with cortical surface area and volume of all regions in the occipital lobe, as well as with thickness, surface area, and volume of the middle temporal

cortex, banks of the superior temporal sulcus, fusiform, supra-marginal and precuneus regions, areas associated with discrimination and recognition of language or visual form. These variants are either intergenic between *KIAA0586*, the product of which is a conserved centrosomal protein essential for ciliogenesis, sonic hedgehog signaling and intracellular organization, and *DACT1*, the product of which is a target for *SIRT1* and acts on the wnt/ β -catenin pathway. *KIAA0586* has been associated with Joubert syndrome, another condition associated with abnormal cerebellar development. Other variants are intergenic between *DACT1* and *DAAMI* or intronic in *DAAMI*. *DAAMI* has been associated with occipital lobe volume in a previous GWAS³¹.

Locus 6q22.32 contains various SNPs associated with cortical surface area and volume globally, and also within some frontal, temporal and occipital regions. The SNPs are intergenic between *RSPO3* and *CENPW*. *RSPO3* and *CENPW* have been previously associated with intracranial^{32,33} and occipital lobe volumes³¹. *RSPO3* is an activator of the canonical Wnt signaling pathway and a regulator of angiogenesis.

Chr17q21.31 variants were associated with global cortical surface area and volume and with regions in temporal lobe. These variants are intronic in the genes *PLEKHM1*, *CRHR1*, *NSF*, and *WNT3*. In previous GWAS analyses, these genes have been associated with general cognitive function³⁴ and neuroticism³⁵. *CRHR1*, *NSF*, and *WNT3* were additionally associated with Parkinson's disease³⁶ and intracranial volume^{32,33,37}. The *NSF* gene also plays a role in Neuronal Intranuclear Inclusion Disease³⁸ and *CRHR1* is involved in anxiety and depressive disorders³⁹. This chromosomal region also contains the *MAPT* gene, which plays a role in Alzheimer's disease, Parkinson's disease, and fronto-temporal dementia^{40,41}.

The protein product of the gene *ZIC4* is a C2H2 zinc finger transcription factor that has an intraneuronal, non-synaptic expression and auto-antibodies to this protein have been associated with subacute sensory neuronopathy, limbic encephalitis, and seizures in patients with breast, small cell lung or ovarian cancers. *ZIC4* null mice have abnormal development of the visual pathway⁴² and heterozygous deletion of the gene has also been associated with a congenital cerebellar (Dandy-Walker) malformation⁴³, thus implicating it widely in brain development as well as in neurodegeneration. *C2H2ZF* transcription factors are the most widely expressed transcription factors in eukaryotes and show associations with responses to abiotic (environmental) stressors. Another transcription factor, *FOXCl*, also associated with Dandy-Walker syndrome has been previously shown to be associated with risk of all types of ischemic stroke and with stroke

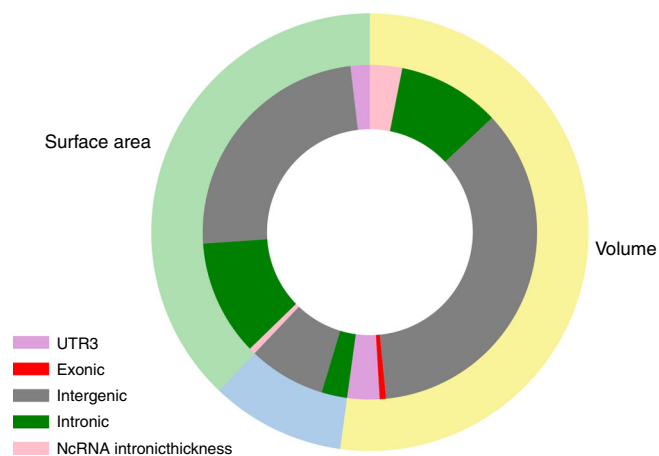


Fig. 3 Functional annotation categories for global and regional CTh, CSA, and CV. Proportion of functional annotation categories for global and regional cortical thickness (blue), surface area (light green), and volume (yellow) assigned by ANNOVAR.

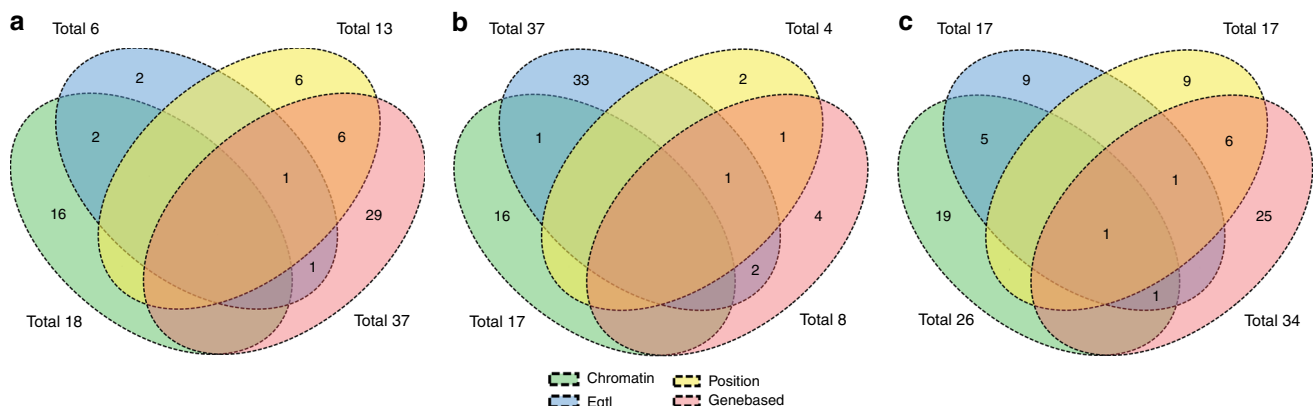


Fig. 4 Number of overlapping genes between gene mapping methods. Number of overlapping genes between FUMA eQTL mapping, FUMA chromatin interaction mapping, ANNOVAR chromosome positional mapping, and MAGMA gene-based analysis for all cortical regions combined for cortical surface area (a), thickness (b) and volume (c).

severity. Thus, *ZIC4* might be a biological target worth pursuing to ameliorate neurodegenerative disorders.

We found an exonic SNP within the gene *ENPP2* (Autotaxin) at 8q24.12 to be associated with insular cortical volume. This gene is differentially expressed in the frontal cortex of Alzheimer patients⁴⁴ and in mouse models of Alzheimer disease, such as the senescence-accelerated mouse prone 8 strain (SAMP8) mouse. Autotaxin is a dual-function ectoenzyme, which is the primary source of the signaling lipid, lysophosphatidic acid. Besides Alzheimer disease, changes in autotaxin/lysophosphatidic acid signaling have also been shown in diverse brain-related conditions, such as intractable pain, pruritus, glioblastoma, multiple sclerosis, and schizophrenia. In the SAMP8 mouse, improvements in cognition noted after administration of LW-AFC, a putative Alzheimer remedy derived from the traditional Chinese medicinal prescription ‘Liuwei Dihuang’ decoction, are correlated with restored expression of four genes in the hippocampus, one of which is *ENPP2*.

Among the other genetic regions identified, many have been linked to neurological and psychiatric disorders, cognitive functioning, cortical development, and cerebral structure (detailed listing in Supplementary Data 31).

Heritability estimates are, as expected, generally higher in the family-based Austrian Stroke Prevention-Family study (ASPS-Fam) than in the Rotterdam Study (RS) for CTh (average $h^2_{\text{ASPS-Fam}} = 0.52$; $h^2_{\text{RS}} = 0.26$), CSA (0.62 and 0.30) and CV (0.57 and 0.23). This discrepancy is explained by the different heritability estimation methods: pedigree-based heritability in ASPS-Fam versus heritability based on common SNPs that are in LD with causal variants⁴⁵ in RS.

Average heritability over regions is also higher for surface area and volume, than for thickness. The observed greater heritability of CSA compared to CTh is consistent with the previously articulated hypothesis, albeit based on much smaller numbers, that CSA is developmentally determined to a greater extent with smaller subsequent decline after young adulthood, whereas CTh changes over the lifespan as aging, neurodegeneration and vascular injuries accrue^{1,3}. It is also interesting that brain regions more susceptible to early amyloid deposition (e.g., superior temporal cortex and precuneus) have a higher heritability.

We found no or weak genetic correlation between CTh and CSA, globally and regionally, and no common lead SNPs, which indicates that these two morphological measures are genetically independent, a finding consistent with prior reports^{15,16}. In contrast, we found strong genetic correlation between CSA and CV and identified common lead SNPs for CSA and CV globally, and in 12 cortical regions. Similar findings have been reported in a previous publication¹⁶. The genetic correlation between CTh and CV ranged between 0.09 and 0.77, implying a common genetic background in some regions (such as the primary sensory postcentral and lingual cortices), but not in others. For CTh, we observed genetic correlations between multiple regions within each of the lobes, whereas for CSA and CV, we found genetic correlations mainly between different regions of the occipital lobe. Chen et al.⁴⁶ have also reported strong genetic correlation for CSA within the occipital lobe. There were also a few genetic correlations observed for regions from different lobes, suggesting similarities in cortical development transcended traditional lobar boundaries.

A limitation of our study is the heterogeneity of the MR phenotypes between cohorts due to different scanners, field strengths, MR protocols and MRI analysis software. This heterogeneity as well as the different age ranges in the participating cohorts may have caused different effects over the cohorts. We nevertheless combined the data of the individual cohorts to maximize the sample size as it has been done in previous

CHARGE GWAS analyses^{31–33}. To account for the heterogeneity we used a sample-size weighted meta-analysis that does not provide overall effect estimates. This method has lower power to detect associations compared to inverse-variance weighted meta-analysis and we therefore may have found less associations. Our inability to replicate 8 of the 76 genome-wide significant findings for CTh and CSA could be caused by false-positive results but may also be explained by insufficient power due to a too small sample size. Moreover, our sample comprises of mainly European ancestry, limiting the generalizability to other ethnicities. Strengths of our study are the population-based design, the large age range of our sample (20–100 years), use of three cortical measures as phenotypes of cortical morphometry, and the replication of our CTh and CSA findings in a large and independent cohort. In conclusion, we identified patterns of heritability and genetic associations with various global and regional cortical measures, as well as overlap of MRI cortical measures with genetic traits and diseases that provide new insights into cortical development, morphology, and possible mechanisms of disease susceptibility.

Methods

Study population. The sample of this study consist of up to 22,824 participants from 20 population-based cohort studies collaborating in the Cohorts of Heart and Aging Research in Genomic Epidemiology (CHARGE) consortium and the UK Biobank (UKBB). All the individuals were stroke- and dementia free, aged between 20 and 100 years, and of European ancestry, except for ARIC AA with African ancestry. Supplementary Data 32 provides population characteristics of each cohort and the Supplementary Methods provide a short description of each study. Each study secured approval from institutional review boards or equivalent organizations, and all participants provided written informed consent. Our results were replicated using summary GWAS findings of 22,635 individuals from the ENIGMA consortium.

Genotyping and imputation. Genotyping was conducted using various commercially available genotyping arrays across the study cohorts. Prior to imputation, extensive quality control was performed in each cohort. Genotype data were imputed to the 1000 Genomes reference panel (mainly phase 1, version 3) using validated software. Details on genotyping, quality control and imputation can be found in Supplementary Data 33.

Phenotype definition. This study investigated CTh, CSA, and CV globally in the whole cortex and in 34 cortical regions. Global and regional CTh was defined as the mean thickness of the left and the right hemisphere in millimeter (mm). Global CSA was defined as the total surface area of the left and the right hemisphere in mm^2 , while regional CSA was defined as the mean surface area of the left and the right hemisphere in mm^2 . Global and regional CV was defined as the mean volume of the left and the right hemisphere in mm^3 . The 34 cortical regions are listed in the Supplementary Methods. High resolution brain magnetic resonance imaging (MRI) data was obtained in each cohort using a range of MRI scanners, field strengths and protocols. CTh, CSA, and CV were generated using the Freesurfer software package⁴⁷ in all cohorts except for FHSucl, where an in-house segmentation method was used. MRI protocols of each cohort can be found in Supplementary Data 35 and descriptive statistics of CTh, CSA, and CV can be found in Supplementary Data 36–38.

Genome-wide association analysis. Based on a predefined analysis plan, each study fitted linear regression models to determine the association between global and regional CTh, CSA, and CV and allele dosages of SNPs. Additive genetic effects were assumed and the models were adjusted for sex, age, age², and if needed for study site and for principal components to correct for population stratification. Cohorts including related individuals calculated linear mixed models to account for family structure. Details on association software and covariates for each cohort are shown in Supplementary Data 33. Models investigating regional CTh, CSA, and CV were additionally adjusted for global CTh, global CSA and global CV, respectively. Quality control of the summary statistics shared by each cohort was performed using EasyQC⁴⁸. Genetic variants with a minor allele frequency (MAF) <0.05, low imputation quality ($R^2 < 0.4$), and which were available in less than 10,000 individuals were removed from the analyses. Details on quality control are provided in the Supplementary Methods.

We then used METAL⁴⁹ to perform meta-analyses using the z -scores method, based on p -values, sample size, and direction of effect, with genomic control correction. To estimate the number of independent tests for the p -value threshold correction, we used a non-parametric permutation testing procedure^{50–53} in the

combined Rotterdam Study cohort ($N = 4442$) and UK Biobank ($N = 8213$). First, we generated a random independent variable, to insure that there is no true relationship between brain measurements and this variable. Second, we ran linear regression analyses between this variable and all brain measurements one-by-one in each of the cohorts separately (104 regressions in total per cohort). Third, we saved the minimum p -value obtained from those 104 regressions. Then, as suggested in literature⁵⁴, we repeated this procedure 10,000 times. Therefore, at the end we had 10,000 minimum p -values per cohort. The minimum p -value distribution follows a Beta distribution $Beta(m, n)$, where $m = 1$ and n is the degree of freedom, which represents the number of independent tests in case of permutation testing. Using python statistical library we fitted the Beta function with the saved minimum p -values, and found n for Rotterdam Study and UK Biobank identically equal to 46. Based on the permutation test results, the genome-wide significance threshold was set a priori at 1.09×10^{-9} ($=5 \times 10^{-8}/46$). We used the clumping function in PLINK⁵⁵ (linkage disequilibrium (LD) threshold: 0.2, distance: 300 kb) to identify the most significant SNP in each LD block. We used LDSR to calculate genomic inflation factors (λ_{GC}), LDSR intercepts and LDSR ratios for each meta-analysis. The LDSR intercept was estimated to differentiate between inflation due to a polygenic signal and inflation due to population stratification⁵⁶. The LDSR ratio represents the amount of inflation that is due to other causes than polygenicity such as population stratification or cryptic relatedness.

For replication of our genome-wide significant CTh and CSA associations, we used GWAS meta-analysis results from the ENIGMA consortium²² for all SNPs that were associated at a p -value $< 5 \times 10^{-8}$ and performed a pooled meta-analysis. The p -value threshold for replication was set to 3.1×10^{-4} ($=0.05/160$: nominal significance threshold divided by total number of lead SNPs). CV was not available in the ENIGMA results. PRS analysis was performed for 7800 out of sample subjects (not included in the current GWAS) from UK Biobank cohort using the PRSice-2 software⁵⁷ with standard settings. The significance threshold for the association between the PRS and the phenotype was set to 4.76×10^{-3} ($=0.05/105$: nominal significance divided by number GWAS phenotypes). The NHGRI-EBI Catalog of published GWAS⁵⁸ was searched for previous SNP-trait associations at a p -value of 5×10^{-8} of lead SNPs. Regional association plots were generated with LocusZoom⁵⁹, and the chromosomal ideogram with PHENOGRAM (<http://visualization.ritchielab.org/phenograms/plot>).

Annotation of genome-wide significant variants was performed using the ANNOVAR software package⁶⁰ and the FUMA web application⁶¹. FUMA eQTL mapping uses information from three data repositories (GTEx, Blood eQTL browser, and BIOS QTL browser) and maps SNPs to genes based on a significant eQTL association. We used a false discovery rate threshold (FDR) of 0.05 divided by number of tests (46) to define significant eQTL associations. Gene-based analyses, to combine the effects of SNPs assigned to a gene, and gene set analyses, to find out if genes assigned to significant SNPs were involved in biological pathways, were performed using MAGMA⁶² as implemented in FUMA. The significance threshold was set to 5.87×10^{-8} ($=0.05/18522 \times 46$: FDR threshold divided by number of genes and independent tests) for gene-based analyses and to 1.02×10^{-7} ($=0.05/10651$: FDR threshold divided by the number of gene sets) for the gene set analyses. Additionally, FUMA was used to investigate a significant chromatin interaction between a genomic region in a risk locus and promoter regions of genes (250 bp upstream and 500 bp downstream of a TSS). We used an FDR of 1×10^{-6} to define significant interactions.

We investigated cis (< 1 Mb) and trans (> 1 Mb or on a different chromosome) expression quantitative trait loci (eQTL) for genome-wide significant SNPs in 724 post-mortem brains from ROSMAP^{63,64} stored in the AMP-AD database. The samples were collected from the gray matter of the dorsolateral prefrontal cortex. The significance threshold was set to 0.001 ($=0.05/46$: FDR threshold divided by the number of independent tests). For additional pathway analyses of genes that were mapped to independent lead SNPs by FUMA, we searched the InnateDB database⁶⁵. The STRING database⁶⁶ was used for visualizing protein-protein interactions. Only those protein subnetworks with five or more nodes are shown.

Heritability. Additive genetic heritability (h^2) of CTh, CSA, and CV was estimated in two studies: the Austrian Stroke Prevention Family Study (ASPS-Fam; $n = 365$) and the Rotterdam Study (RS, $n = 4472$). In the population-based family study ASPS-Fam, the ratio of the genotypic variance to the phenotypic variance was calculated using variance components models in SOLAR⁶⁷. In case of non-normality, phenotype data were inverse-normal transformed. In RS, SNP-based heritability was computed with GCTA⁶⁸. These heritability analyses were adjusted for age and sex.

Heritability and partitioned heritability based on GWAS summary statistics was calculated from GWAS summary statistics using LDSR implemented in the LDSC tool (<https://github.com/bulik/ldsc>). Partitioned heritability analysis splits genome-wide SNP heritability into 53 functional annotation classes (e.g., coding, 3'UTR, promoter, transcription factor binding sites, conserved regions etc.) and additionally to 10 cell-type specific classes (e.g., central nervous system, cardiovascular, liver, skeletal muscle, etc.) as defined by Finucane et al.⁶⁹ to estimate their contributions to heritability. The significance threshold was set to 2.05×10^{-5} ($=0.05/53 \times 46$: nominal significance divided by number of functional annotation classes and number of independent tests) for heritability partitioned on

functional annotation classes and $2.05 < 10^{-6}$ ($=0.05/53 \times 10 \times 46$: nominal significance divided by number of functional annotation classes, number of cell types and number of independent tests) for heritability partitioned on annotation classes and cell types.

Genetic correlation. LDSR genetic correlation⁷⁰ between CTh, CSA, and CV was estimated globally and within each cortical region. The significance threshold was set to 7.35×10^{-4} (nominal threshold (0.05) divided by number of regions (34) and by number of correlations (CSA and CV, CSA and CTh)). Genetic correlation was also estimated between all 34 cortical regions for CTh, CSA, and CV, with the significance threshold set to 8.91×10^{-5} (nominal threshold (0.05) divided by number of regions (34) times the number of regions -1 (33) divided by 2 (half of the matrix)). Additionally, the amount of genetic correlation was quantified between CTh, CSA, and CV and physical traits (height, body mass index), neurological and psychiatric diseases (e.g., Alzheimer's disease, Parkinson's disease), cognitive traits and MRI volumes (p -value threshold (0.05/46/number of GWAS traits)). As recommended by the LDSC tool developers, only HapMap3 variants were included in these analyses, as these tend to be well-imputed across cohorts.

Reporting summary. Further information on research design is available in the Nature Research Reporting Summary linked to this article.

Data availability

The genome-wide summary statistics that support the findings of this study are available via the CHARGE Summary Results portal at the NCBI dbGaP website <https://www.omicsci.org/dataset/dbgap/phs000930> upon publication, or from the corresponding authors R.S. and S.S. upon reasonable request. The summary statistics may be used for all scientific purposes except for the study of potentially sensitive and potentially stereotyping phenotypes such as intelligence and addiction, since this is proscribed by the consent terms for the NHLBI cohorts. Individual level data or study-specific summary results are only available through controlled access. Data for the Framingham Study are available through dbGaP, where qualified researchers can apply for authorization to access (https://www.ncbi.nlm.nih.gov/projects/gap/cgi-bin/study.cgi?study_id=phs000007.v30.p11). Individual level data for the ARIC and CHS studies are also available through dbGaP. Data of European and Australian cohorts are available upon request, in keeping with data sharing guidelines in the EU General Data Protection Regulation. Data from UK Biobank can be accessed at <http://www.ukbiobank.ac.uk> and for the ENIGMA consortium from medlandse@gmail.com. Individual level data for VETSA is not available due to consent restrictions.

Received: 4 March 2020; Accepted: 20 August 2020;

Published online: 22 September 2020

References

- Storsve, A. B. et al. Differential longitudinal changes in cortical thickness, surface area and volume across the adult life span: regions of accelerating and decelerating change. *J. Neurosci.* **34**, 8488–8498 (2014).
- Hogstrom, L. J., Westlye, L. T., Walhovd, K. B. & Fjell, A. M. The structure of the cerebral cortex across adult life: age-related patterns of surface area, thickness, and gyrification. *Cereb. Cortex* **23**, 2521–2530 (2013).
- Fjell, A. M. et al. Development and aging of cortical thickness correspond to genetic organization patterns. *Proc. Natl Acad. Sci. USA* **112**, 15462–15467 (2015).
- Vuoksimaa, E. et al. The genetic association between neocortical volume and general cognitive ability is driven by global surface area rather than thickness. *Cereb. Cortex* **25**, 2127–2137 (2015).
- Vuoksimaa, E. et al. Is bigger always better? The importance of cortical configuration with respect to cognitive ability. *NeuroImage* **129**, 356–366 (2016).
- Lerch, J. P. et al. Focal decline of cortical thickness in Alzheimer's disease identified by computational neuroanatomy. *Cereb. Cortex* **15**, 995–1001 (2005).
- Uribe, C. et al. Patterns of cortical thinning in nondemented Parkinson's disease patients. *Mov. Disord.* **31**, 699–708 (2016).
- Steenwijk, M. D. et al. Cortical atrophy patterns in multiple sclerosis are non-random and clinically relevant. *Brain* **139**, 115–126 (2016).
- Rimol, L. M. et al. Cortical volume, surface area, and thickness in schizophrenia and bipolar disorder. *Biol. Psychiatry* **71**, 552–560 (2012).
- Schmaal, L. et al. Cortical abnormalities in adults and adolescents with major depression based on brain scans from 20 cohorts worldwide in the ENIGMA Major Depressive Disorder Working Group. *Mol. Psychiatry* **22**, 900–909 (2017).
- van Rooij, D. et al. Cortical and subcortical brain morphometry differences between patients with autism spectrum disorder and healthy individuals

- across the lifespan: results from the ENIGMA ASD Working Group. *Am. J. Psychiatry* **175**, 359–369 (2018).
12. Mountcastle, V. B. The columnar organization of the neocortex. *Brain* **120**(Pt 4), 701–722 (1997).
 13. Rakic, P. A small step for the cell, a giant leap for mankind: a hypothesis of neocortical expansion during evolution. *Trends Neurosci.* **18**, 383–388 (1995).
 14. Rakic, P. Evolution of the neocortex: a perspective from developmental biology. *Nat. Rev. Neurosci.* **10**, 724–735 (2009).
 15. Panizzon, M. S. et al. Distinct genetic influences on cortical surface area and cortical thickness. *Cereb. Cortex* **19**, 2728–2735 (2009).
 16. Winkler, A. M. et al. Cortical thickness or grey matter volume? The importance of selecting the phenotype for imaging genetics studies. *NeuroImage* **53**, 1135–1146 (2010).
 17. Rimol, L. M. et al. Cortical thickness is influenced by regionally specific genetic factors. *Biol. Psychiatry* **67**, 493–499 (2010).
 18. Eyer, L. T. et al. Genetic and environmental contributions to regional cortical surface area in humans: a magnetic resonance imaging twin study. *Cereb. Cortex* **21**, 2313–2321 (2011).
 19. Kremen, W. S. et al. Genetic and environmental influences on the size of specific brain regions in midlife: the VETSA MRI study. *Neuroimage* **49**, 1213–1223 (2010).
 20. Joshi, A. A. et al. The contribution of genes to cortical thickness and volume. *Neuroreport* **22**, 101–105 (2011).
 21. Wen, W. et al. Distinct genetic influences on cortical and subcortical brain structures. *Sci. Rep.* **6**, 32760 (2016).
 22. Grasby, K. L. et al. The genetic architecture of the human cerebral cortex. *Science*. <https://doi.org/10.1126/science.aay6690> (2020).
 23. Elliott, L. T. et al. Genome-wide association studies of brain imaging phenotypes in UK Biobank. *Nature* **562**, 210–216 (2018).
 24. Zhao, B. et al. Genome-wide association analysis of 19,629 individuals identifies variants influencing regional brain volumes and refines their genetic co-architecture with cognitive and mental health traits. *Nat. Genet.* **51**, 1637–1644 (2019).
 25. Hibar, D. P. et al. Novel genetic loci associated with hippocampal volume. *Nat. Commun.* **8**, 13624 (2017).
 26. Irvin, M. R. et al. Genome-wide meta-analysis of SNP-by-9-ACEI/ARB and SNP-by-thiazide diuretic and effect on serum potassium in cohorts of European and African ancestry. *Pharmacogenomics J.* <https://doi.org/10.1038/s41397-018-0021-9> (2018).
 27. Lu, L. et al. Common and rare variants of the THBS1 gene associated with the risk for autism. *Psychiatr. Genet.* **24**, 235–240 (2014).
 28. Park, H. J., Kim, S. K., Kim, J. W., Kang, W. S. & Chung, J. H. Association of thrombospondin 1 gene with schizophrenia in Korean population. *Mol. Biol. Rep.* **39**, 6875–6880 (2012).
 29. Christopherson, K. S. et al. Thrombospondins are astrocyte-secreted proteins that promote CNS synaptogenesis. *Cell* **120**, 421–433 (2005).
 30. Blake, S. M. et al. Thrombospondin-1 binds to ApoER2 and VLDL receptor and functions in postnatal neuronal migration. *EMBO J.* **27**, 3069–3080 (2008).
 31. van der Lee, S. J. et al. A genome-wide association study identifies genetic loci associated with specific lobar brain volumes. *Commun. Biol.* **2**, 285 (2019).
 32. Ikram, M. A. et al. Common variants at 6q22 and 17q21 are associated with intracranial volume. *Nat. Genet.* **44**, 539–544 (2012).
 33. Adams, H. H. et al. Novel genetic loci underlying human intracranial volume identified through genome-wide association. *Nat. Neurosci.* **19**, 1569–1582 (2016).
 34. Davies, G. et al. Study of 300,486 individuals identifies 148 independent genetic loci influencing general cognitive function. *Nat. Commun.* **9**, 2098 (2018).
 35. Luciano, M. et al. Association analysis in over 329,000 individuals identifies 116 independent variants influencing neuroticism. *Nat. Genet.* **50**, 6–11 (2018).
 36. Chang, D. et al. A meta-analysis of genome-wide association studies identifies 17 new Parkinson's disease risk loci. *Nat. Genet.* **49**, 1511–1516 (2017).
 37. Hibar, D. P. et al. Common genetic variants influence human subcortical brain structures. *Nature* **520**, 224–229 (2015).
 38. Pountney, D. L., Raftery, M. J., Chegini, F., Blumbergs, P. C. & Gai, W. P. NSF, Unc-18-1, dynamin-1 and HSP90 are inclusion body components in neuronal intranuclear inclusion disease identified by anti-SUMO-1-immunocapture. *Acta Neuropathologica* **116**, 603–614 (2008).
 39. Muller, M. B. & Wurst, W. Getting closer to affective disorders: the role of CRH receptor systems. *Trends Mol. Med.* **10**, 409–415 (2004).
 40. Desikan, R. S. et al. Genetic overlap between Alzheimer's disease and Parkinson's disease at the MAPT locus. *Mol. Psychiatry* **20**, 1588–1595 (2015).
 41. Spillantini, M. G. & Goedert, M. Tau pathology and neurodegeneration. *Lancet Neurol.* **12**, 609–622 (2013).
 42. Horng, S. et al. Differential gene expression in the developing lateral geniculate nucleus and medial geniculate nucleus reveals novel roles for Zic4 and Foxp2 in visual and auditory pathway development. *The. J. Neurosci.* **29**, 13672–13683 (2009).
 43. Grinberg, I. et al. Heterozygous deletion of the linked genes ZIC1 and ZIC4 is involved in Dandy-Walker malformation. *Nat. Genet.* **36**, 1053–1055 (2004).
 44. Umemura, K. et al. Autotaxin expression is enhanced in frontal cortex of Alzheimer-type dementia patients. *Neurosci. Lett.* **400**, 97–100 (2006).
 45. Wray, N. R. et al. Pitfalls of predicting complex traits from SNPs. *Nat. Rev. Genet.* **14**, 507–515 (2013).
 46. Chen, C. H. et al. Genetic influences on cortical regionalization in the human brain. *Neuron* **72**, 537–544 (2011).
 47. Desikan, R. S. et al. An automated labeling system for subdividing the human cerebral cortex on MRI scans into gyral based regions of interest. *Neuroimage* **31**, 968–980 (2006).
 48. Winkler, T. W. et al. Quality control and conduct of genome-wide association meta-analyses. *Nat. Protoc.* **9**, 1192–1212 (2014).
 49. Willer, C. J., Li, Y. & Abecasis, G. R. METAL: fast and efficient meta-analysis of genomewide association scans. *Bioinformatics* **26**, 2190–2191 (2010).
 50. Purcell, S. et al. PLINK: a tool set for whole-genome association and population-based linkage analyses. *Am. J. Hum. Genet.* **81**, 559–575 (2007).
 51. Nichols, T. E. Multiple testing corrections, nonparametric methods, and random field theory. *NeuroImage* **62**, 811–815 (2012).
 52. Uppu, S., Krishna, A. & Gopalan, R. P. A review on methods for detecting SNP interactions in high-dimensional genomic. *Data. IEEE/ACM Trans. Comput. Biol. Bioinform.* **15**, 599–612 (2018).
 53. Alberton, B. A. V., Nichols, T. E., Gamba, H. R. & Winkler, A. M. Multiple testing correction over contrasts for brain imaging. *NeuroImage*. <https://doi.org/10.1016/j.neuroimage.2020.116760> (2020).
 54. Churchill, G. A. & Doerge, R. W. Empirical threshold values for quantitative trait mapping. *Genetics* **138**, 963–971 (1994).
 55. Chang, C. C. et al. Second-generation PLINK: rising to the challenge of larger and richer datasets. *GigaScience* **4**, 7 (2015).
 56. Bulik-Sullivan, B. K. et al. LD Score regression distinguishes confounding from polygenicity in genome-wide association studies. *Nat. Genet.* **47**, 291–295 (2015).
 57. Choi, S. W. & O'Reilly, P. F. PRSice-2: Polygenic Risk Score software for biobank-scale data. *Gigascience* <https://doi.org/10.1093/gigascience/giz082> (2019).
 58. MacArthur, J. et al. The new NHGRI-EBI Catalog of published genome-wide association studies (GWAS Catalog). *Nucleic Acids Res.* **45**, D896–D901 (2017).
 59. Pruim, R. J. et al. LocusZoom: regional visualization of genome-wide association scan results. *Bioinformatics* **26**, 2336–2337 (2010).
 60. Wang, K., Li, M. & Hakonarson, H. ANNOVAR: functional annotation of genetic variants from high-throughput sequencing data. *Nucleic Acids Res.* **38**, e164 (2010).
 61. Watanabe, K., Taskesen, E., van Bochoven, A. & Posthuma, D. Functional mapping and annotation of genetic associations with FUMA. *Nat. Commun.* **8**, 1826 (2017).
 62. de Leeuw, C. A., Mooij, J. M., Heskes, T. & Posthuma, D. MAGMA: generalized gene-set analysis of GWAS data. *PLoS Comput Biol.* **11**, e1004219 (2015).
 63. Bennett, D. A., Schneider, J. A., Arvanitakis, Z. & Wilson, R. S. Overview and findings from the religious orders study. *Curr. Alzheimer Res.* **9**, 628–645 (2012).
 64. Bennett, D. A. et al. Overview and findings from the rush Memory and Aging Project. *Curr. Alzheimer Res.* **9**, 646–663 (2012).
 65. Breuer, K. et al. InnateDB: systems biology of innate immunity and beyond—recent updates and continuing curation. *Nucleic acids Res.* **41**, D1228–D1233 (2013).
 66. Szklarczyk, D. et al. The STRING database in 2017: quality-controlled protein-protein association networks, made broadly accessible. *Nucleic acids Res.* **45**, D362–D368 (2017).
 67. Almasy, L. & Blangero, J. Multipoint quantitative-trait linkage analysis in general pedigrees. *Am. J. Hum. Genet.* **62**, 1198–1211 (1998).
 68. Yang, J., Lee, S. H., Goddard, M. E. & Visscher, P. M. GCTA: a tool for genome-wide complex trait analysis. *Am. J. Hum. Genet.* **88**, 76–82 (2011).
 69. Finucane, H. K. et al. Partitioning heritability by functional annotation using genome-wide association summary statistics. *Nat. Genet.* **47**, 1228–1235 (2015).
 70. Bulik-Sullivan, B. et al. An atlas of genetic correlations across human diseases and traits. *Nat. Genet.* **47**, 1236–1241 (2015).

Acknowledgements

We provide all investigator and study-specific acknowledgements in Supplementary Note 1.

Author contributions

Drafting of the manuscript: E.H., G.V.R., R.S., and S.S.; Genotype and phenotype data acquisition: H.S., N.A., P.R.S., M.J.W., C.E.F., P.S.S., K.A.M., N.J.A., J.B.K., O.A.A., A.M.D., M.C.N., U.V., R.S., S.M., B.M., J.J., J.T., G.B.P., H.B., A.T., D.A., R.B., J.T.B., O.L.L., C.T., and P.A.; Imaging, genetic and bioinformatics analysis: E.H., G.V.R., H.H.H.A., M.J.K., Y.S., R.X., J.C.B., S.A., S.L., S.J.v.d.L., Q.Y., C.L.S., H.L., J.J.H., H.Z., M.L., M.S., N.J.A., M.W.V., A.T., K.W., M.B., A.M., N.A.G., M.L., P.R.S., X.J., O.C., A.S.B., L.P., St. S., P.M., C.d.C., S.K., L.L., M.B., W.W., F.B., A.V.W., M.H., J.J., and F.C. Cohort PIs: P.S.S., W.S.K., J.A.W., A.V., C.M.v. D., H.J.G., W.T.L.Jr., M.F., T.P., S.D., M.A.I., H.S., R.S., S.S., J.I.R., B.M.P., I.J.D., M.L., A.H., A.G.U., W.J.N., Z.P., M.S.P., T.H.M., J.T., C.E.F., M.J.L., and C.T.; ENIGMA Study design: K.L.G., N.J., J.N.P., L.C.-C., J.B., D.P.H., P.A.L., F.P., J.L.S., P.M.T., and S.E.M.; Critical revision of the manuscript: all authors.

Competing interests

Dr. Dale is a founder of and holds equity in CorTechs Labs, Inc, and serves on its Scientific Advisory Board. He is a member of the Scientific Advisory Board of Human Longevity, Inc. and receives funding through research agreements with General Electric Healthcare and Medtronic, Inc. The terms of these arrangements have been reviewed and approved by UCSD in accordance with its conflict of interest policies. W. Niessen is co-founder and shareholder of Quantib BV. H. Brodaty is an advisory board member of Nutricia. The other authors declare no competing interests.

Additional information

Supplementary information is available for this paper at <https://doi.org/10.1038/s41467-020-18367-y>.

Correspondence and requests for materials should be addressed to R.S. or S.S.

Peer review information *Nature Communications* thanks the anonymous reviewers for their contribution to the peer review of this work. Peer review reports are available.

Reprints and permission information is available at <http://www.nature.com/reprints>

Publisher's note Springer Nature remains neutral with regard to jurisdictional claims in published maps and institutional affiliations.



Open Access This article is licensed under a Creative Commons Attribution 4.0 International License, which permits use, sharing, adaptation, distribution and reproduction in any medium or format, as long as you give appropriate credit to the original author(s) and the source, provide a link to the Creative Commons license, and indicate if changes were made. The images or other third party material in this article are included in the article's Creative Commons license, unless indicated otherwise in a credit line to the material. If material is not included in the article's Creative Commons license and your intended use is not permitted by statutory regulation or exceeds the permitted use, you will need to obtain permission directly from the copyright holder. To view a copy of this license, visit <http://creativecommons.org/licenses/by/4.0/>.

© The Author(s) 2020

Edith Hofer^{1,2,229}, Gennady V. Roshchupkin^{3,4,5,229}, Hieab H. H. Adams^{3,5,229}, Maria J. Knof⁵, Honghuang Lin⁶, Shuo Li⁷, Habil Zare^{8,9}, Shahzad Ahmad⁵, Nicola J. Armstrong¹⁰, Claudia L. Satizabal^{8,11}, Manon Bernard¹², Joshua C. Bis¹³, Nathan A. Gillespie^{14,15}, Michelle Luciano^{16,17}, Aniket Mishra¹⁸, Markus Scholz^{19,20}, Alexander Teumer²¹, Rui Xia²², Xueqiu Jian²², Thomas H. Mosley²³, Yasaman Saba²⁴, Lukas Pirpamer¹, Stephan Seiler^{25,26}, James T. Becker²⁷, Owen Carmichael²⁸, Jerome I. Rotter²⁹, Bruce M. Psaty¹³, Oscar L. Lopez²⁷, Najaf Amin⁵, Sven J. van der Lee⁵, Qiong Yang⁷, Jayandra J. Himali⁷, Pauline Maillard^{25,26}, Alexa S. Beiser^{7,11}, Charles DeCarli^{25,26}, Sherif Karama³⁰, Lindsay Lewis³⁰, Mat Harris^{16,31,32,33}, Mark E. Bastin^{16,31,32,33}, Ian J. Deary^{16,17}, A. Veronica Witte^{34,35}, Frauke Beyer^{34,35}, Markus Loeffler^{19,20}, Karen A. Mather^{36,37}, Peter R. Schofield^{37,38}, Anbupalam Thalamuthu³⁶, John B. Kwok^{38,39}, Margaret J. Wright^{40,41}, David Ames^{42,43}, Julian Trollor^{36,44}, Jiyang Jiang³⁶, Henry Brodaty^{45,36}, Wei Wen³⁶, Meike W. Vernooij^{3,5}, Albert Hofman^{46,5}, André G. Uitterlinden⁵, Wiro J. Niessen^{47,3}, Katharina Wittfeld^{48,49}, Robin Bülow⁵⁰, Uwe Völker⁵¹, Zdenka Pausova^{12,52}, G. Bruce Pike⁵³, Sophie Maingault⁵⁴, Fabrice Crivello⁵⁴, Christophe Tzourio^{18,55}, Philippe Amouyel^{56,57,58}, Bernard Mazoyer⁵⁴, Michael C. Neale¹⁴, Carol E. Franz⁵⁹, Michael J. Lyons⁶⁰, Matthew S. Panizzon⁵⁹, Ole A. Andreassen⁶¹, Anders M. Dale⁶², Mark Logue^{7,63,64}, Katrina L. Grasby⁶⁵, Neda Jahanshad⁶⁶, Jodie N. Painter⁶⁵, Lucía Colodro-Conde⁶⁵, Janita Bralten^{67,68}, Derrek P. Hibar^{66,69}, Penelope A. Lind⁶⁵, Fabrizio Pizzagalli⁶⁶, Jason L. Stein⁷⁰, Paul M. Thompson⁶⁶, Sarah E. Medland⁶⁵, ENIGMA consortium*, Perminder S. Sachdev^{36,71}, William S. Kremen⁵⁹, Joanna M. Wardlaw^{16,31,32,33}, Arno Villringer^{34,72}, Cornelia M. van Duijn^{5,73}, Hans J. Grabe^{48,49}, William T. Longstreth Jr⁷⁴, Myriam Fornage²², Tomas Paus^{75,76}, Stephanie Debette^{11,18,77}, M. Arfan Ikram^{3,5,78}, Helena Schmidt²⁴, Reinhold Schmidt^{1,230} & Sudha Seshadri^{8,11,230}

¹Clinical Division of Neurogeriatrics, Department of Neurology, Medical University of Graz, Graz, Austria. ²Institute for Medical Informatics, Statistics and Documentation, Medical University of Graz, Graz, Austria. ³Department of Radiology and Nuclear Medicine, Erasmus MC, Rotterdam, The Netherlands. ⁴Department of Medical Informatics, Erasmus MC, Rotterdam, The Netherlands. ⁵Department of Epidemiology, Erasmus MC, Rotterdam, The Netherlands. ⁶Section of Computational Biomedicine, Department of Medicine, Boston University School of

Medicine, Boston, MA, USA. ⁷Department of Biostatistics, Boston University School of Public Health, Boston, MA, USA. ⁸Glenn Biggs Institute for Alzheimer's and Neurodegenerative Diseases, UT Health San Antonio, San Antonio, USA. ⁹Department of Cell Systems & Anatomy, The University of Texas Health Science Center, San Antonio, TX, USA. ¹⁰Mathematics and Statistics, Murdoch University, Perth, Australia. ¹¹Department of Neurology, Boston University School of Medicine, Boston, MA, USA. ¹²Hospital for Sick Children, Toronto, ON, Canada. ¹³Cardiovascular Health Research Unit, Department of Medicine, Epidemiology and Health Services, University of Washington, Seattle, WA, USA. ¹⁴Virginia Institute for Psychiatric and Behavior Genetics, Virginia Commonwealth University, Richmond, VA, USA. ¹⁵QIMR Berghofer Medical Research Institute, Herston, QLD, Australia. ¹⁶Centre for Cognitive Epidemiology and Cognitive Ageing, University of Edinburgh, Edinburgh, UK. ¹⁷Department of Psychology, University of Edinburgh, Edinburgh, UK. ¹⁸University of Bordeaux, Bordeaux Population Health Research Center, INSERM UMR 1219, Bordeaux, France. ¹⁹Institute for Medical Informatics, Statistics and Epidemiology, University of Leipzig, Leipzig, Germany. ²⁰LIFE Research Center for Civilization Diseases, University of Leipzig, Leipzig, Germany. ²¹Institute for Community Medicine, University Medicine Greifswald, Greifswald, Germany. ²²Institute of Molecular Medicine and Human Genetics Center, University of Texas Health Science Center at Houston, Houston, TX, USA. ²³Department of Medicine, University of Mississippi Medical Center, Jackson, MS, USA. ²⁴Gottfried Schatz Research Center for Cell Signaling, Metabolism and Aging, Medical University of Graz, Graz, Austria. ²⁵Imaging of Dementia and Aging (IDEA) Laboratory, Department of Neurology, University of California-Davis, Davis, CA, USA. ²⁶Department of Neurology and Center for Neuroscience, University of California at Davis, Sacramento, CA, USA. ²⁷Departments of Psychiatry, Neurology, and Psychology, University of Pittsburgh, Pittsburgh, PA, USA. ²⁸Pennington Biomedical Research Center, Baton Rouge, LA, USA. ²⁹Institute for Translational Genomics and Population Sciences, Los Angeles Biomedical Research Institute and Pediatrics at Harbor-UCLA Medical Center, Torrance, CA, USA. ³⁰McGill University, Montreal Neurological Institute, Montreal, QC, Canada. ³¹Centre for Clinical Brain Sciences, University of Edinburgh, Edinburgh, UK. ³²Brain Research Imaging Centre, University of Edinburgh, Edinburgh, UK. ³³Scottish Imaging Network, A Platform for Scientific Excellence (SINAPSE) Collaboration, Department of Neuroimaging Sciences, The University of Edinburgh, Edinburgh, UK. ³⁴Department of Neurology, Max Planck Institute for Human Cognitive and Brain Sciences, Leipzig, Germany. ³⁵Faculty of Medicine, CRC 1052 Obesity Mechanisms, University of Leipzig, Leipzig, Germany. ³⁶Centre for Healthy Brain Ageing, School of Psychiatry, University of New South Wales, Sydney, Australia. ³⁷Neuroscience Research Australia, Sydney, Australia. ³⁸School of Medical Sciences, University of New South Wales, Sydney, Australia. ³⁹Brain and Mind Centre - The University of Sydney, Camperdown, NSW, Australia. ⁴⁰Queensland Brain Institute, The University of Queensland, St Lucia, QLD, Australia. ⁴¹Centre for Advanced Imaging, The University of Queensland, St Lucia, QLD, Australia. ⁴²National Ageing Research Institute, Royal Melbourne Hospital, Parkville, VIC, Australia. ⁴³Academic Unit for Psychiatry of Old Age, University of Melbourne, St George's Hospital, Kew, VIC, Australia. ⁴⁴Department of Developmental Disability Neuropsychiatry, School of Psychiatry, University of New South Wales, Sydney, NSW, Australia. ⁴⁵Dementia Centre for Research Collaboration, University of New South Wales, Sydney, NSW, Australia. ⁴⁶Department of Epidemiology, Harvard T.H. Chan School of Public Health, Boston, MA, USA. ⁴⁷Imaging Physics, Faculty of Applied Sciences, Delft University of Technology, Delft, The Netherlands. ⁴⁸German Center for Neurodegenerative Diseases (DZNE), Site Rostock/Greifswald, Greifswald, Germany. ⁴⁹Department of Psychiatry and Psychotherapy, University Medicine Greifswald, Greifswald, Germany. ⁵⁰Institute for Diagnostic Radiology and Neuroradiology, University Medicine Greifswald, Greifswald, Germany. ⁵¹Interfaculty Institute for Genetics and Functional Genomics, University Medicine Greifswald, Greifswald, Germany. ⁵²Departments of Physiology and Nutritional Sciences, University of Toronto, Toronto, ON, Canada. ⁵³Departments of Radiology and Clinical Neurosciences, University of Calgary, Calgary, AB, Canada. ⁵⁴Institut des Maladies Neurodégénératives UMR5293, CEA, CNRS, University of Bordeaux, Bordeaux, France. ⁵⁵Pole de santé publique, Centre Hospitalier Universitaire de Bordeaux, Bordeaux, France. ⁵⁶Centre Hospitalier Universitaire de Bordeaux, France; Inserm U1167, Lille, France. ⁵⁷Department of Epidemiology and Public Health, Pasteur Institute of Lille, Lille, France. ⁵⁸Department of Public Health, Lille University Hospital, Lille, France. ⁵⁹Department of Psychiatry, University of California San Diego, San Diego, CA, USA. ⁶⁰Department of Psychological and Brain Sciences, Boston University, Boston, MA, USA. ⁶¹NORMENT, KG Jebsen Centre for Psychosis Research, Institute of Clinical Medicine, University of Oslo and Division of Mental Health and Addiction, Oslo University Hospital, Oslo, Norway. ⁶²Departments of Radiology and Neurosciences, University of California, San Diego, La Jolla, CA, USA. ⁶³National Center for PTSD at Boston VA Healthcare System, Boston, MA, USA. ⁶⁴Department of Psychiatry and Department of Medicine-Biomedical Genetics Section, Boston University School of Medicine, Boston, MA, USA. ⁶⁵Psychiatric Genetics, QIMR Berghofer Medical Research Institute, Brisbane, QLD, Australia. ⁶⁶Imaging Genetics Center, Mark and Mary Stevens Neuroimaging and Informatics Institute, Keck School of Medicine of USC, University of Southern California, Los Angeles, CA, USA. ⁶⁷Department of Human Genetics, Radboud university medical center, Nijmegen, The Netherlands. ⁶⁸Donders Institute for Brain, Cognition and Behaviour, Radboud University, Nijmegen, The Netherlands. ⁶⁹Neuroscience Biomarkers, Janssen Research and Development, LLC, San Diego, CA, USA. ⁷⁰Department of Genetics & UNC Neuroscience Center, University of North Carolina at Chapel Hill, Chapel Hill, NC, USA. ⁷¹Neuropsychiatric Institute, Prince of Wales Hospital, Sydney, NSW, Australia. ⁷²Day Clinic for Cognitive Neurology, University Hospital Leipzig, Leipzig, Germany. ⁷³Nuffield Department of Population Health, University of Oxford, Oxford, UK. ⁷⁴Departments of Neurology and Epidemiology, University of Washington, Seattle, WA, USA. ⁷⁵Bloorview Research Institute, Holland Bloorview Kids Rehabilitation Hospital, Toronto, ON, Canada. ⁷⁶Departments of Psychology and Psychiatry, University of Toronto, Toronto, ON, Canada. ⁷⁷CHU de Bordeaux, Department of Neurology, F-33000 Bordeaux, France. ⁷⁸Department of Neurology, Erasmus MC, Rotterdam, The Netherlands. ²²⁹These authors contributed equally: Edith Hofer, Gennady V. Roshchupkin, Hieab H.H. Adams. ²³⁰These authors jointly supervised this work: Reinhold Schmidt, Sudha Seshadri. *A list of authors and their affiliations appears at the end of the paper. [✉]email: reinhold.schmidt@medunigraz.at; suseshad@bu.edu

ENIGMA consortium

Katrina L. Grasby⁷⁹, Neda Jahanshad⁸⁰, Jodie N. Painter⁷⁹, Lucía Colodro-Conde⁷⁹, Janita Bralten^{81,82}, Derrek P. Hibar^{80,83}, Penelope A. Lind⁷⁹, Fabrizio Pizzagalli⁸⁰, Christopher R. K. Ching⁸⁰, Mary Agnes B. McMahon⁸⁰, Natalia Shatkhina⁸⁰, Leo C. P. Zsembik⁸⁴, Ingrid Agartz⁸⁵, Saud Alhusaini⁸⁶, Marcio A. A. Almeida⁸⁷, Dag Alnæs⁸⁵, Inge K. Amlien⁸⁸, Micael Andersson⁸⁹, Tyler Ard⁸⁰, Nicola J. Armstrong⁸⁸, Allison Ashley-Koch⁹⁰, Manon Bernard⁹¹, Rachel M. Brouwer⁹², Elizabeth E. L. Buimer⁹², Robin Bülow⁹³, Christian Bürger⁹⁴, Dara M. Cannon⁹⁵, Mallar Chakravarty⁹⁶, Qiang Chen⁹⁷, Joshua W. Cheung⁸⁰, Baptiste Couvy-Duchesne⁹⁸, Anders M. Dale⁹⁹, Shareefa Dalvie¹⁰⁰, Tânia K. de Araujo¹⁰¹,

Greig I. de Zubizaray¹⁰², Sonja M. C. de Zwarte⁹², Anouk den Braber¹⁰³, Nhat Trung Doan⁸⁵, Katharina Dohm⁹⁴, Stefan Ehrlich¹⁰⁴, Hannah-Ruth Engelbrecht¹⁰⁵, Susanne Erk¹⁰⁶, Chun Chieh Fan¹⁰⁷, Iryna O. Fedko¹⁰³, Sonya F. Foley¹⁰⁸, Judith M. Ford¹⁰⁹, Masaki Fukunaga¹¹⁰, Melanie E. Garrett⁹⁰, Tian Ge¹¹¹, Sudheer Giddaluru¹¹², Aaron L. Goldman⁹⁷, Nynke A. Groenewold¹⁰⁰, Dominik Grotegerd⁹⁴, Tiril P. Gurholt⁸⁵, Boris A. Gutman⁸⁰, Narelle K. Hansell¹¹³, Mathew A. Harris^{114,115,116,117}, Marc B. Harrison⁸⁰, Courtney C. Haswell¹¹⁸, Michael Hauser⁹⁰, Stefan Herms¹¹⁹, Dirk J. Heslenfeld¹²⁰, New Fei Ho¹²¹, David Hoehn¹²², Per Hoffmann¹¹⁹, Laurena Holleran⁹⁵, Martine Hoogman⁸¹, Jouke-Jan Hottenga¹⁰³, Masashi Ikeda¹²³, Deborah Janowitz¹²⁴, Iris E. Jansen¹²⁵, Tianye Jia¹²⁶, Christiane Jockwitz¹²⁷, Ryota Kanai¹²⁸, Sherif Karama¹²⁹, Dalia Kasperaviciute¹³⁰, Tobias Kaufmann⁸⁵, Sinead Kelly¹³¹, Masataka Kikuchi¹³², Marieke Klein⁸¹, Michael Knapp¹³³, Annchen R. Knodt¹³⁴, Bernd Krämer¹³⁵, Max Lam¹²¹, Thomas M. Lancaster¹⁰⁸, Phil H. Lee¹¹¹, Tristram A. Lett¹⁰⁶, Lindsay B. Lewis¹²⁹, Iscia Lopes-Cendes¹⁰¹, Michelle Luciano^{114,136}, Fabio Macciardi¹³⁷, Andre F. Marquand¹³⁸, Samuel R. Mathias¹³⁹, Tracy R. Melzer¹⁴⁰, Yuri Milaneschi¹⁴¹, Nazanin Mirza-Schreiber¹²², Jose C. V. Moreira¹⁴², Thomas W. Mühleisen¹²⁷, Bertram Müller-Myhsok¹²², Pablo Najt⁹⁵, Soichiro Nakahara¹³⁷, Kwangsik Nho¹⁴³, Loes M. Olde Loohuis¹⁴⁴, Dimitri Papadopoulos Orfanos¹⁴⁵, John F. Pearson¹⁴⁶, Toni L. Pitcher¹⁴⁰, Benno Pütz¹²², Anjanibhargavi Ragothaman⁸⁰, Faisal M. Rashid⁸⁰, Ronny Redlich⁹⁴, Céline S. Reinbold¹¹⁹, Jonathan Repple⁹⁴, Geneviève Richard⁸⁵, Brandalyn C. Riedel⁸⁰, Shannon L. Risacher¹⁴³, Cristiane S. Rocha¹⁰¹, Nina Roth Mota⁸¹, Lauren Salminen⁸⁰, Arvin Saremi⁸⁰, Andrew J. Saykin¹⁴³, Fenja Schlag¹⁴⁷, Lianne Schmaal¹⁴⁸, Peter R. Schofield^{149,150}, Rodrigo Secolin¹⁰¹, Chin Yang Shapland¹⁴⁷, Li Shen¹⁵¹, Jean Shin⁹¹, Elena Shumskaya⁸¹, Ida E. Sønderby⁸⁵, Emma Sprooten⁸², Lachlan T. Strike¹¹³, Katherine E. Tansey¹⁵², Alexander Teumer¹⁵³, Anbupalam Thalamuthu¹⁵⁴, Sophia I. Thomopoulos⁸⁰, Diana Tordesillas-Gutiérrez¹⁵⁵, Jessica A. Turner¹⁵⁶, Anne Uhlmann¹⁰⁰, Costanza Ludovica Vallerga⁹⁸, Dennis van der Meer⁸⁵, Marjolein M. J. van Donkelaar⁸¹, Liza van Eijk¹⁵⁷, Theo G. M. van Erp¹³⁷, Neeltje E. M. van Haren⁹², Daan van Rooij¹³⁸, Marie-José van Tol¹⁵⁸, Jan H. Veldink¹⁵⁹, Ellen Verhoef¹⁴⁷, Esther Walton¹⁵⁶, Mingyuan Wang¹²¹, Yunpeng Wang⁸⁵, Joanna M. Wardlaw^{114,115,116,117}, Wei Wen¹⁵⁴, Lars T. Westlye⁸⁵, Christopher D. Whelan⁸⁰, Stephanie H. Witt¹⁶⁰, Katharina Wittfeld^{161,124}, Christiane Wolf¹⁶², Thomas Wolfers⁸¹, Clarissa L. Yasuda¹⁶³, Dario Zaremba⁹⁴, Zuo Zhang¹⁶⁴, Alyssa H. Zhu⁸⁰, Marcel P. Zwiers¹³⁸, Eric Artiges¹⁶⁵, Amelia A. Assareh¹⁵⁴, Rosa Ayesa-Arriola¹⁶⁶, Aysenil Belger¹¹⁸, Christine L. Brandt⁸⁵, Gregory G. Brown¹⁶⁷, Sven Cichon¹¹⁹, Joanne E. Curran⁸⁷, Gareth E. Davies¹⁶⁸, Franziska Degenhardt¹⁶⁹, Bruno Dietsche¹⁷⁰, Srdjan Djurovic¹⁷¹, Colin P. Doherty¹⁷², Ryan Espiritu¹⁷³, Daniel Garijo¹⁷³, Yolanda Gil¹⁷³, Penny A. Gowland¹⁷⁴, Robert C. Green¹⁷⁵, Alexander N. Häusler¹⁷⁶, Walter Heindel¹⁷⁷, Beng-Choon Ho¹⁷⁸, Wolfgang U. Hoffmann¹⁵³, Florian Holsboer¹⁷⁹, Georg Homuth¹⁸⁰, Norbert Hosten⁹³, Clifford R. Jack Jr¹⁸¹, MiHyun Jang¹⁷³, Andreas Jansen¹⁷⁰, Knut Kolaskar¹⁶³, Sanne Koops⁹², Axel Krug¹⁷⁰, Kelvin O. Lim¹⁸², Jurjen J. Luyckx¹⁸³, Daniel H. Mathalon¹⁸⁴, Karen A. Mather¹⁵⁴, Venkata S. Mattay⁹⁷, Sarah Matthews¹⁸⁵, Jaqueline Mayoral Van Son¹⁶⁶, Sarah C. McEwen¹⁶⁷, Ingrid Melle¹⁶³, Derek W. Morris¹⁷³, Bryon A. Mueller¹⁸², Matthias Nauck¹⁸⁶, Jan E. Nordvik¹⁸⁷, Markus M. Nöthen¹⁶⁹, Daniel S. O'Leary¹⁷⁸, Nils Opel⁹⁴, Marie -. Laure Paillère Martinot¹⁶⁵, G. Bruce Pike¹⁸⁸, Adrian Preda¹³⁷, Erin B. Quinlan¹⁶⁴, Varun Ratnakar¹⁷³, Simone Reppermund¹⁵⁴, Vidar M. Steen¹¹², Fábio R. Torres¹⁰¹, Dick J. Veltman¹⁴¹, James T. Voyvodich¹¹⁸, Robert Whelan¹⁸⁹, Tonya White¹⁹⁰, Hidenaga Yamamori¹⁹¹, Marina K. M. Alvim¹⁶³, David Ames^{192,193}, Tim J. Anderson¹⁴⁰, Ole A. Andreassen⁸⁵, Alejandro Arias-Vasquez¹⁹⁴, Mark E. Bastin^{114,115,116,117}, Bernhard T. Baune¹⁹⁵, John Blangero⁸⁷, Dorret I. Boomsma¹⁰³, Henry Brodaty¹⁵⁴, Han G. Brunner⁸¹, Randy L. Buckner¹⁹⁶, Jan K. Buitelaar¹³⁸, Juan R. Bustillo¹⁹⁷, Wiepke Cahn⁹², Vince Calhoun¹⁹⁸, Xavier Caseras¹⁵², Svenja Caspers¹⁹⁹, Gianpiero L. Cavalleri⁸⁶, Fernando Cendes¹⁶³, Aiden Corvin²⁰⁰, Benedicto Crespo-Facorro¹⁶⁶, John C. Dalrymple-Alford²⁰¹, Udo Dannlowski⁹⁴, Eco J. C. de Geus¹⁰³, Ian J. Deary^{114,136}, Norman Delanty²⁰²,

Chantal Depondt²⁰³, Sylvane Desrivieres¹⁶⁴, Gary Donohoe⁹⁵, Thomas Espeseth²⁰⁴, Guillén Fernández¹³⁸, Simon E. Fisher¹⁴⁷, Herta Flor²⁰⁵, Andreas J. Forstner¹⁶⁹, Clyde Francks¹⁴⁷, Barbara Franke⁸¹, David C. Glahn¹³⁹, Randy L. Gollub²⁰⁶, Hans J. Grabe^{161,124}, Oliver Gruber¹³⁵, Asta K. Häberg²⁰⁷, Ahmad R. Hariri¹³⁴, Catharina A. Hartman²⁰⁸, Ryota Hashimoto²⁰⁹, Andreas Heinz¹⁰⁶, Manon H. J. Hillegers¹⁹⁰, Pieter J. Hoekstra²⁰⁸, Avram J. Holmes¹³⁹, L. Elliot Hong²¹⁰, William D. Hopkins²¹¹, Hilleke E. Hulshoff Pol⁹², Terry L. Jernigan²¹², Erik G. Jönsson²¹³, René S. Kahn²¹⁴, Martin A. Kennedy²¹⁵, Tilo T. J. Kircher¹⁷⁰, Peter Kochunov²¹⁰, John B. J. Kwok^{150,216}, Stephanie Le Hellard¹¹², Nicholas G. Martin⁷⁹, Jean -. Luc Martinot¹⁶⁵, Colm McDonald⁹⁵, Katie L. McMahon²¹⁷, Andreas Meyer-Lindenberg²¹⁸, Rajendra A. Morey¹¹⁸, Lars Nyberg⁸⁹, Jaap Oosterlaan²¹⁹, Roel A. Ophoff¹⁴⁴, Tomáš Paus^{220,221}, Zdenka Pausova^{91,222}, Brenda W. J. H. Penninx¹⁴¹, Tinca J. C. Polderman¹²⁵, Danielle Posthuma¹²⁵, Marcella Rietschel¹⁶⁰, Joshua L. Roffman²⁰⁶, Laura M. Rowland²¹⁰, Perminder S. Sachdev¹⁵⁴, Philipp G. Sämann¹²², Gunter Schumann¹⁶⁴, Kang Sim²²³, Sanjay M. Sisodiya²⁰⁸, Jordan W. Smoller¹¹¹, Iris E. Sommer²²⁴, Beate St Pourcain¹⁸⁵, Dan J. Stein¹⁰⁰, Arthur W. Toga⁸⁰, Julian N. Trollor^{154,225}, Nic J. A. Van der Wee²²⁶, Dennis van 't Ent¹⁰³, Henry Völzke¹⁵³, Henrik Walter¹⁰⁶, Bernd Weber²²⁷, Daniel R. Weinberger⁹⁷, Margaret J. Wright¹¹³, Juan Zhou²²⁸, Jason L. Stein⁸⁴, Paul M. Thompson⁸⁰ & Sarah E. Medland⁷⁹

⁷⁹Psychiatric Genetics, QIMR Berghofer Medical Research Institute, Brisbane, QLD, Australia. ⁸⁰Imaging Genetics Center, Mark and Mary Stevens Neuroimaging and Informatics Institute, Keck School of Medicine of USC, University of Southern California, Los Angeles, CA, USA. ⁸¹Department of Human Genetics, Radboud university medical center, Nijmegen, The Netherlands. ⁸²Donders Institute for Brain, Cognition and Behaviour, Radboud University, Nijmegen, The Netherlands. ⁸³Neuroscience Biomarkers, Janssen Research and Development, LLC, San Diego, CA, USA. ⁸⁴Department of Genetics & UNC Neuroscience Center, University of North Carolina at Chapel Hill, Chapel Hill, NC, USA. ⁸⁵NORMENT, KG Jebsen Centre for Psychosis Research, Institute of Clinical Medicine, University of Oslo and Division of Mental Health and Addiction, Oslo University Hospital, Oslo, Norway. ⁸⁶Department of Molecular and Cellular Therapeutics, Royal College of Surgeons in Ireland, Dublin, Ireland. ⁸⁷Department of Human Genetics and South Texas Diabetes and Obesity Institute, Rio Grande Valley School of Medicine, University of Texas, Brownsville, USA. ⁸⁸Centre for Lifespan Changes in Brain and Cognition, Department of Psychology, University of Oslo, Oslo, Norway. ⁸⁹Department of Integrative Medical Biology, Umeå University, Umeå, Sweden. ⁹⁰Duke Molecular Physiology Institute, Duke University Medical Center, Durham, NC, USA. ⁹¹Hospital for Sick Children, Toronto, ON, Canada. ⁹²Department of Psychiatry, Brain Center Rudolf Magnus, University Medical Center Utrecht, Utrecht University, Utrecht, The Netherlands. ⁹³Institute for Diagnostic Radiology and Neuroradiology, University Medicine Greifswald, Greifswald, Germany. ⁹⁴Department of Psychiatry, University of Münster, Münster, Germany. ⁹⁵Centre for Neuroimaging & Cognitive Genomics, National University of Ireland Galway, Galway, Ireland. ⁹⁶Douglas Mental Health University Institute, McGill University, Montreal, QC, Canada. ⁹⁷Lieber Institute for Brain Development, Baltimore, MD, USA. ⁹⁸Institute for Molecular Bioscience, The University of Queensland, Brisbane, QLD, Australia. ⁹⁹Departments of Radiology and Neurosciences, University of California, San Diego, La Jolla, CA, USA. ¹⁰⁰Department of Psychiatry and Mental Health, University of Cape Town, Cape Town, South Africa. ¹⁰¹Department of Medical Genetics, School of Medical Sciences, University of Campinas - UNICAMP, Campinas, Brazil. ¹⁰²Faculty of Health, Institute of Health and Biomedical Innovation, Queensland University of Technology, Brisbane, QLD, Australia. ¹⁰³Department of Biological Psychology, Vrije Universiteit Amsterdam, Amsterdam, The Netherlands. ¹⁰⁴Division of Psychological & Social Medicine and Developmental Neurosciences, Technische Universität Dresden, Dresden, Germany. ¹⁰⁵Division of Human Genetics, Institute of Infectious Disease and Molecular Medicine, University of Cape Town, Cape Town, South Africa. ¹⁰⁶Division of Mind and Brain Research, Department of Psychiatry and Psychotherapy, Campus Charité Mitte, Charité - Universitätsmedizin Berlin, Berlin, Germany. ¹⁰⁷Department of Cognitive Science, University of California San Diego, San Diego, CA, USA. ¹⁰⁸Cardiff University Brain Research Imaging Centre, Cardiff University, Cardiff, UK. ¹⁰⁹San Francisco Veterans Administration Medical Center, San Francisco, CA, USA. ¹¹⁰Division of Cerebral Integration, National Institute for Physiological Sciences, Okazaki, Japan. ¹¹¹Psychiatric and Neurodevelopmental Genetics Unit, Center for Genomic Medicine, Massachusetts General Hospital, Boston, MA, USA. ¹¹²NORMENT - K.G. Jebsen Centre for Psychosis Research, Department of Clinical Science, NORMENT University of Bergen, Bergen, Norway. ¹¹³Queensland Brain Institute, The University of Queensland, St Lucia, QLD, Australia. ¹¹⁴Centre for Cognitive Epidemiology and Cognitive Ageing, University of Edinburgh, Edinburgh, UK. ¹¹⁵Centre for Clinical Brain Sciences, University of Edinburgh, Edinburgh, UK. ¹¹⁶Brain Research Imaging Centre, University of Edinburgh, Edinburgh, UK. ¹¹⁷Scottish Imaging Network, A Platform for Scientific Excellence (SINAPSE) Collaboration, Department of Neuroimaging Sciences, The University of Edinburgh, Edinburgh, UK. ¹¹⁸Duke UNC Brain Imaging and Analysis Center, Duke University Medical Center, Durham, NC, USA. ¹¹⁹Department of Biomedicine, University of Basel, Basel, Switzerland. ¹²⁰Department of Cognitive and Clinical Neuropsychology, Vrije Universiteit Amsterdam, Amsterdam, The Netherlands. ¹²¹Research Division, Institute of Mental Health, Singapore, Singapore. ¹²²Max Planck Institute of Psychiatry, Munich, Germany. ¹²³Department of Psychiatry, Fujita Health University School of Medicine, Toyooka, Japan. ¹²⁴Department of Psychiatry and Psychotherapy, University Medicine Greifswald, Greifswald, Germany. ¹²⁵Complex Trait Genetics, Center for Neurogenomics and Cognitive Research, Vrije Universiteit Amsterdam, Amsterdam, The Netherlands. ¹²⁶Institute of Science and Technology for Brain-Inspired Intelligence, Fudan University, Shanghai, China. ¹²⁷Institute of Neuroscience and Medicine (INM-1), Research Centre Jülich, Jülich, Germany. ¹²⁸Department of Neuroinformatics, Araya, Inc, Tokyo, Japan. ¹²⁹McGill University, Montreal Neurological Institute, Montreal, QC, Canada. ¹³⁰Department of Clinical and Experimental Epilepsy, UCL Institute of Neurology, London, UK. ¹³¹Public Psychiatry Division, Massachusetts Mental Health Center, Beth Israel Deaconess Medical Center, Harvard Medical School, Boston, MA, USA. ¹³²Department of Genome Informatics, Graduate School of Medicine, Osaka University, Suita, Japan. ¹³³Department of Medical Biometry, Informatics and Epidemiology, University Hospital Bonn, Bonn, Germany. ¹³⁴Department of Psychology and Neuroscience, Duke University, Durham, NC, USA. ¹³⁵Section for Experimental Psychopathology and Neuroimaging, Department of General Psychiatry, Heidelberg University Hospital, Heidelberg, Germany. ¹³⁶Department of Psychology, University of Edinburgh, Edinburgh, UK. ¹³⁷Department of Psychiatry and Human Behavior, School of Medicine, University of California, Irvine, Irvine, CA, USA. ¹³⁸Department of Cognitive

Neuroscience, Radboud university medical center, Nijmegen, The Netherlands. ¹³⁹Department of Psychiatry, Yale University School of Medicine, New Haven, CT, USA. ¹⁴⁰Department of Medicine, University of Otago, Christchurch, Christchurch, New Zealand. ¹⁴¹Psychiatry, Amsterdam UMC Vrije Universiteit, Amsterdam, The Netherlands. ¹⁴²BRAINN - Brazilian Institute of Neuroscience and Neurotechnology, Campinas, Brazil. ¹⁴³Department of Radiology and Imaging Sciences, Indiana University School of Medicine, Indianapolis, IN, USA. ¹⁴⁴Center for Neurobehavioral Genetics, University of California Los Angeles, Los Angeles, CA, USA. ¹⁴⁵NeuroSpin, CEA, Université Paris-Saclay, Gif sur Yvette, France. ¹⁴⁶Biostatistics and Computational Biology Unit, University of Otago, Christchurch, Christchurch, New Zealand. ¹⁴⁷Language and Genetics Department, Max Planck Institute for Psycholinguistics, Nijmegen, The Netherlands. ¹⁴⁸Orygen, The National Centre of Excellence for Youth Mental Health, Melbourne, Australia. ¹⁴⁹Neuroscience Research Australia, Sydney, NSW, Australia. ¹⁵⁰School of Medical Sciences, University of New South Wales, Sydney, NSW, Australia. ¹⁵¹Department of Biostatistics, Epidemiology and Informatics, University of Pennsylvania, Philadelphia, PA, USA. ¹⁵²MRC Centre for Neuropsychiatric Genetics and Genomics, Cardiff University, Cardiff, UK. ¹⁵³Institute for Community Medicine, University Medicine Greifswald, Greifswald, Germany. ¹⁵⁴Centre for Healthy Brain Ageing, School of Psychiatry, University of New South Wales, Sydney, NSW, Australia. ¹⁵⁵Neuroimaging Unit, Valdecilla Biomedical Research Institute IDIVAL, Santander, Spain. ¹⁵⁶Department of Psychology, Georgia State University, Atlanta, GA, USA. ¹⁵⁷School of Psychology, University of Queensland, Brisbane, QLD, Australia. ¹⁵⁸Cognitive Neuroscience Center, Department of Neuroscience, University Medical Center Groningen, Groningen, The Netherlands. ¹⁵⁹Department of Neurology, Brain Center Rudolf Magnus, University Medical Center Utrecht, Utrecht University, Utrecht, The Netherlands. ¹⁶⁰Department of Genetic Epidemiology in Psychiatry, Central Institute of Mental Health, Medical Faculty Mannheim, Heidelberg University, Mannheim, Germany. ¹⁶¹German Center for Neurodegenerative Diseases (DZNE), Site Rostock/ Greifswald, Greifswald, Germany. ¹⁶²Department of Psychiatry, Psychosomatics and Psychotherapy, University of Würzburg, Würzburg, Germany. ¹⁶³Department of Neurology, FCM, University of Campinas - UNICAMP, Campinas, Brazil. ¹⁶⁴Social, Genetic and Developmental Psychiatry Centre, Institute of Psychiatry, Psychology & Neuroscience, King's College London, London, UK. ¹⁶⁵INSERM Unit 1000 - Neuroimaging & Psychiatry, Paris Saclay University, Gif sur Yvette, France. ¹⁶⁶Department of Psychiatry, University Hospital Marqués de Valdecilla, School of Medicine, University of Cantabria-IDIVAL, Santander, Spain. ¹⁶⁷Department of Psychiatry, University of California San Diego, San Diego, CA, USA. ¹⁶⁸Avera Institute for Human Genetics, Sioux Falls, SD, USA. ¹⁶⁹Institute of Human Genetics, School of Medicine & University Hospital Bonn, University of Bonn, Bonn, Germany. ¹⁷⁰Department of Psychiatry and Psychotherapy, Philipps-University Marburg, Marburg, Germany. ¹⁷¹Department of Medical Genetics, Oslo University Hospital, Oslo, Norway. ¹⁷²Department of Neurology, St James's Hospital, Dublin, Ireland. ¹⁷³Information Sciences Institute, University of Southern California, Los Angeles, CA, USA. ¹⁷⁴Sir Peter Mansfield Imaging Centre, University of Nottingham, Nottingham, UK. ¹⁷⁵Brigham and Women's Hospital, Boston, MA, USA. ¹⁷⁶Center for Economics and Neuroscience, University of Bonn, Bonn, Germany. ¹⁷⁷Department of Clinical Radiology, University of Münster, Münster, Germany. ¹⁷⁸Department of Psychiatry, University of Iowa College of Medicine, Iowa City, IA, USA. ¹⁷⁹HMNC Holding GmbH, Munich, Germany. ¹⁸⁰Interfaculty Institute for Genetics and Functional Genomics, University Medicine Greifswald, Greifswald, Germany. ¹⁸¹Department of Radiology, Mayo Clinic, Rochester, MN, USA. ¹⁸²Department of Psychiatry, University of Minnesota, Minneapolis, MN, USA. ¹⁸³Department of Translational Neuroscience, Brain Center Rudolf Magnus, University Medical Center Utrecht, Utrecht University, Utrecht, The Netherlands. ¹⁸⁴Department of Psychiatry and Weill Institute for Neurosciences, University of California San Francisco, San Francisco, CA, USA. ¹⁸⁵MRC Integrative Epidemiology Unit, Department of Population Health Sciences, Bristol Medical School, Bristol, UK. ¹⁸⁶Institute of Clinical Chemistry and Laboratory Medicine, University Medicine Greifswald, Greifswald, Germany. ¹⁸⁷Sunnaas Rehabilitation Hospital HT, Nesodden, Norway. ¹⁸⁸Departments of Radiology and Clinical Neurosciences, University of Calgary, Calgary, AB, Canada. ¹⁸⁹School of Psychology, Trinity College Dublin, Dublin, Ireland. ¹⁹⁰Department of Child and Adolescent Psychiatry/Psychology, Erasmus Medical Center-Sophia Children's Hospital, Rotterdam, The Netherlands. ¹⁹¹Department of Psychiatry, Osaka University Graduate School of Medicine, Suita, Japan. ¹⁹²National Ageing Research Institute, Royal Melbourne Hospital, Parkville, VIC, Australia. ¹⁹³Academic Unit for Psychiatry of Old Age, University of Melbourne, St George's Hospital, Kew, VIC, Australia. ¹⁹⁴Department of Psychiatry, Radboud university medical center, Nijmegen, The Netherlands. ¹⁹⁵Department of Psychiatry, The University of Melbourne, Melbourne, VIC, Australia. ¹⁹⁶Department of Psychology and Center for Brain Science, Harvard University, Boston, MA, USA. ¹⁹⁷Department of Psychiatry, University of New Mexico, Albuquerque, NM, USA. ¹⁹⁸Department of Electrical and Computer Engineering, The University of New Mexico, Albuquerque, NM, USA. ¹⁹⁹Institute for Anatomy I Medical Faculty, Heinrich-Heine University, Düsseldorf, Germany. ²⁰⁰Department of Psychiatry, School of Medicine, Trinity College Dublin, Dublin, Ireland. ²⁰¹Department of Psychology, University of Canterbury, Christchurch, New Zealand. ²⁰²FutureNeuro Research Centre, Royal College of Surgeons in Ireland, Dublin, Ireland. ²⁰³Department of Neurology, Hôpital Erasme, Université Libre de Bruxelles, Brussels, Belgium. ²⁰⁴Department of Psychology, University of Oslo, Oslo, Norway. ²⁰⁵Department of Cognitive and Clinical Neuroscience, Central Institute of Mental Health, Medical Faculty Mannheim, Heidelberg University, Mannheim, Germany. ²⁰⁶Department of Psychiatry, Massachusetts General Hospital, Boston, MA, USA. ²⁰⁷Department of Neuroscience, Norwegian University of Science and Technology, Trondheim, Norway. ²⁰⁸Department of Psychiatry, University Medical Center Groningen, University of Groningen, Groningen, The Netherlands. ²⁰⁹Molecular Research Center for Children's Mental Development, United Graduate School of Child Development, Osaka University, Suita, Japan. ²¹⁰Department of Psychiatry, Maryland Psychiatry Research Center, University of Maryland School of Medicine, Baltimore, MD, USA. ²¹¹Neuroscience Institute, Georgia State University, Atlanta, GA, USA. ²¹²Center for Human Development, University of California San Diego, La Jolla, CA, USA. ²¹³Centre for Psychiatric Research, Department of Clinical Neuroscience, Karolinska Institutet, Stockholm, Sweden. ²¹⁴Department of Psychiatry, Icahn School of Medicine at Mount Sinai, New York, NY, USA. ²¹⁵Department of Pathology and Biomedical Science, University of Otago, Christchurch, Christchurch, New Zealand. ²¹⁶Brain and Mind Centre - The University of Sydney, Camperdown, NSW, Australia. ²¹⁷Herston Imaging Research Facility, School of Clinical Sciences, Queensland University of Technology, Brisbane, QLD, Australia. ²¹⁸Department of Psychiatry and Psychotherapy, Central Institute of Mental Health, Medical Faculty Mannheim, Heidelberg University, Mannheim, Germany. ²¹⁹Emma Children's Hospital, Academic Medical Center, Amsterdam, The Netherlands. ²²⁰Bloorview Research Institute, Holland Bloorview Kids Rehabilitation Hospital, Toronto, ON, Canada. ²²¹Departments of Psychology and Psychiatry, University of Toronto, Toronto, ON, Canada. ²²²Departments of Physiology and Nutritional Sciences, University of Toronto, Toronto, ON, Canada. ²²³General Psychiatry, Institute of Mental Health, Singapore, Singapore. ²²⁴Department of Medical and Biological Psychology, University of Bergen, Bergen, Norway. ²²⁵Department of Developmental Disability Neuropsychiatry, School of Psychiatry, University of New South Wales, Sydney, NSW, Australia. ²²⁶Department of Psychiatry, Leiden University Medical Center, Leiden, The Netherlands. ²²⁷Institute of Experimental Epileptology and Cognition Research, University Hospital Bonn, Bonn, Germany. ²²⁸Center for Cognitive Neuroscience, Neuroscience and behavioral disorders program, Duke-National University of Singapore Medical School, Singapore, Singapore.